

Original Article

Oncogenic and immunological values of RBM34 in osteosarcoma and its pan-cancer analysis

Wenchao Zhang^{1,2}, Rong He³, Wenbing Cao¹, Dapeng Li¹, Qiping Zheng^{4,5}, Yiming Zhang¹

¹Affiliated Hospital of Jiangsu University, Zhenjiang 212000, Jiangsu, China; ²Affiliated Jintan Hospital of Jiangsu University, Changzhou 213200, Jiangsu, China; ³Department of Oncology, Shanghai Tenth People's Hospital, School of Medicine, Tongji University, Shanghai 200072, China; ⁴Department of Hematological Laboratory Science, Jiangsu Key Laboratory of Medical Science and Laboratory Medicine, School of Medicine, Jiangsu University, Zhenjiang 212000, Jiangsu, China; ⁵Shenzhen Walgenron Bio-Pharm Co. Ltd., Shenzhen 518118, Guangdong, China

Received September 29, 2023; Accepted October 30, 2023; Epub November 15, 2023; Published November 30, 2023

Abstract: RNA binding proteins (RBPs) are increasingly recognized as potential factors influencing the advancement, prognostication, and immune response in various solid tumors. Nevertheless, the comprehensive understanding of RBM34's biological mechanisms within the tumor microenvironment remains incomplete, necessitating further systematic pan-cancer investigations to ascertain its diagnostic, prognostic, and immunological significance. In this study, the TCGA, CCLE, HPA, GTEX, and TARGET databases were employed to analyze the expression abundance and subcellular localization of RBM34 in diverse tumor types. Kaplan-Meier survival analyses were used to investigate the impact of RBM34 on clinical prognosis. We implemented the TISIDB portal, CIBERSORT, and ESTIMATE algorithms to assess the correlation between RBM34 expression and immunomodulators, chemokines, and tumor-infiltrating lymphocytes (TILs) in both pan-cancer and osteosarcoma. The CGP database was applied to evaluate the half-maximal inhibitory concentrations of targeted drugs, while TMB, MSI, and MMR were utilized to predict the efficacy of tumor immunotherapy. Furthermore, an RBM34-derived prognostic index (RDPI) was constructed for osteosarcoma patients and linked to outcomes and immune status. Finally, we examined the modulation of RBM34 knockdown on osteosarcoma proliferation and migration capacity. Our results indicate that RBM34 was predominantly localized in the nucleus and differentially expressed in most human cancer types. Kaplan-Meier curve analysis and Cox regression demonstrated that RBM34 expression affected four survival metrics including overall survival (OS) in multiple tumors and was an independent prognostic factor for osteosarcoma. In immunological characterization, RBM34 expression was significantly associated with pan-cancer immunomodulator-related molecules, lymphocyte subpopulation infiltration, and biomarkers of immunotherapy response. Subsequent in vitro experiments provided additional evidence that the suppression of RBM34 impeded the migratory and invasive capabilities of osteosarcoma. Moreover, the utilization of RDPI demonstrated its reliability in prognosticating patient outcomes and estimating the individual immune landscape. Marked differences in multiple TILs (including naive B cells, CD8+ T cells, resting dendritic cells, and activated CD4+ memory T cells) and cancer-associated fibroblast proportion were observed in diverse RDPI score subgroups. Generally, RBM34 exhibited associations with clinical prognosis, immune infiltration, and immunotherapy across various cancer types, and may also serve as a viable therapeutic target for osteosarcoma.

Keywords: RBM34, osteosarcoma, pan-cancer, immune infiltration, prognosis

Introduction

Osteosarcoma represents the most common primary malignant bone tumor among adolescents and children, with a global incidence of approximately 5 per million [1, 2]. As a highly malignant and aggressive disease, osteosarcoma is initially readily transmitted through the bloodstream, and the resulting pulmonary

metastases are the leading cause of death in patients [3, 4]. Unfortunately, early-stage osteosarcoma is difficult to diagnose promptly due to subtle imaging changes and the lack of obvious specific signs or symptoms [5, 6]. Although the long-term survival rate of localized osteosarcoma has been maintained at over 60% with various treatment modalities such as surgical resection and chemotherapy, the 5-year overall

survival for patients with pulmonary metastases is less than 30% and has not improved until today [7, 8]. Notably, osteosarcoma consists not only of cancer cells but also of a variety of infiltrating immune cells [9]. These tumor-infiltrating immune cells (TICs) recruited into the tumor microenvironment (TME) exert pro- or anti-tumor functions and can profoundly influence tumor biology [10, 11]. Newly approved therapeutic options in recent years, including immune checkpoint inhibitors (ICIs) and Chimeric antigen receptor (CAR)-T cell therapy, have provided new ideas for the treatment of solid tumors, while a large number of patients with osteosarcoma have little or no benefit from monotherapy [12, 13]. Therefore, there is an urgent need to develop accurate and reliable immune-related biomarkers and potential therapeutic targets.

RNA-binding proteins (RBPs) are important participants in cellular life activities, forming a complex regulatory network by linking DNA, RNA, and proteins [14]. The cooperative or independent use of different types of RNA binding domains (RBDs) allows RBPs to increase their binding affinity and specificity to different types of RNA [15]. Classical RBDs include RNA recognition motifs, K-homology domains, zinc finger domains, etc., which are capable of recognizing a wide range of downstream targets and conferring a variety of biological functions to RBPs, such as pre-mRNA selective splicing and RNA stability [16]. RBP affects RNA production, metabolism, and function mainly through post-transcriptional regulation, and also has an important impact on DNA transcription and protein function, thus participating in a wide range of processes such as the regulation of cell survival, death, function, and differentiation [17, 18]. Several studies have shown that the abnormal expression and function of RBP in tumor cells have an important impact on tumor development, drug resistance, immune escape, immunosuppressive microenvironment, and other processes [19-21]. For example, human antigen R (HuR), a ubiquitously expressed RBP, is closely associated with chemotherapeutic response, tumor grade, prognosis, and malignant biological behaviors such as angiogenesis, tumor migration, and invasion in breast, colorectal, and ovarian cancers [22, 23].

The RNA-binding motif (RBM) protein family, a subclass of RBPs primarily identified as involved

in nuclear RNA processing, is now thought to play a key role in regulating a wide range of cellular and physiological processes [24]. For example, RBM10 could bind to intronic regions near mRNA splice sites to regulate selective splicing and gene expression [25]. Research by Sun et al. demonstrated that the lncRNA LINC01977 interacts with RBM39 to promote further nuclear entry of Notch2 and prevent its ubiquitination and degradation, leading to hepatocellular carcinoma (HCC) proliferation, angiogenesis, and EMT [26]. Another study noted that RBMS2, which is lowly expressed in breast cancer, stabilizes P21 mRNA by directly binding to the AU-rich element of the 3'-UTR region to inhibit tumor proliferation and induce cell cycle arrest [27]. As reported by Liu et al., RBM34 was associated with adverse clinicopathological features, immune cell biomarkers, and immune checkpoint expression in HCC, and knockout of RBM34 inhibited the proliferation and migration of HCC cells and increased their sensitivity to sorafenib [28]. However, further systematic investigations across multiple cancer types and the functional role of RBM34 in osteosarcoma remain to be elucidated.

In the present study, we detailed the differential expression of RBM34 in various cancers and analyzed its correlation with immunomodulators, chemokines, lymphocyte subpopulation infiltration, tumor stemness, tumor mutational burden (TMB), microsatellite instability (MSI). We further focused on the independent prognostic value and relevant immune and pharmacogenomic features of RBM34 in osteosarcoma. In addition, we constructed an RBM34-derived prognostic index (RDPI) to predict overall survival (OS), immune function, and cancer-associated fibroblast (CAF) infiltration level of individual patients, providing guidance for therapeutic strategies in osteosarcoma. Overall, our study suggests that RBM34 may serve as a potential prognostic biomarker and therapeutic target for osteosarcoma.

Materials and methods

Sample data collation, differential expression analysis, and subcellular localization analysis

RNA-Seq data, mutation information, and clinical characteristics of 33 tumors were obtained from The Cancer Genome Atlas (TCGA) database (<https://portal.gdc.cancer.gov/>). The

RBM34 as a potential biomarker for osteosarcoma

abbreviations of these above tumors are listed in [Supplementary Table 1](#). The differential RBM34 expression in TCGA pan-cancer samples, including tumor and normal tissues, was assessed using the TIMER database (<https://cistrome.shinyapps.io/timer/>). RBM34 expression profiles in various cancer cell lines were explored using transcriptome data from the CCLE database (<https://portals.broadinstitute.org/ccle/home>). Subsequently, osteosarcoma datasets with complete clinical information and gene expression profiles were downloaded from GEO (with accession number GSE21257) and TARGET databases. Osteosarcoma patients from both cohorts were combined into the osteosarcoma meta-cohort and bias-corrected for batch effects using the “sva” package. After excluding patients with unavailable gene expression matrices, we included data from 141 osteosarcoma cases to ensure the reliability of the study results. A dataset of 396 normal musculoskeletal samples was obtained from the GTEx database (<https://www.gtexportal.org/home/>) as a control [29, 30]. We extracted and visualized the differential expression values of RBM34 between osteosarcoma and control samples with the “limma” and “ggplot2” packages. In addition, we validated the subcellular localization of RBM34 in osteosarcoma by the Human Protein Atlas (HPA) database (www.proteinatlas.org) to promote the understanding of the basic cellular composition.

Prognostic analysis of RBM34

The “survival” and “survminer” packages were used to evaluate the effect of RBM34 in pan-cancer based on four survival metrics, including overall survival (OS), disease-free interval (DFI), progression-free interval (PFI), and disease-specific survival (DSS). As for osteosarcoma, we explored the impact of RBM34 on clinical outcomes through a merged osteosarcoma meta-cohort due to insufficient samples in a single dataset. R2 (<https://hgserver1.amc.nl/cgi-bin/r2/main.cgi>), an online database for genomics analysis, was used to further validate the prognostic significance of RBM34 in osteosarcoma.

Immunological features analysis, immunotherapeutic analysis, tumor stemness analysis, drug susceptibility analysis

We utilized the Tumor-Immune System Interaction Database (TISIDB), ESTIMATE, and

CIBERSORT algorithms to comprehensively explore the potential relationship between RBM34 expression and immune profiling in pan-cancer and osteosarcoma. Specifically, the TISIDB website (<https://cis.hku.hk/TISIDB/index.php>) was used to predict correlations between RBM34 expression and immunomodulators, tumor-infiltrating lymphocytes, and chemokines in pan-cancer. The ESTIMATE algorithm was used to derive ESTIMATE scores, immune scores, stromal scores, and tumor purity to represent the immune status of each tumor. Thereafter, Spearman’s test was performed to explore the relevance of RBM34 expression to the above four indexes with filter criteria of $|\text{correlation coefficient}| > 0.35$ and $P < 0.05$. The CIBERSORT deconvolution algorithm was employed to accurately quantify the proportions of TICs (22 different cell types) according to the gene expression profiles of each tumor sample. The Spearman test was then conducted to investigate the correlation between RBM34 expression and immune cell content with filter criteria of $|\text{correlation coefficient}| > 0.5$ and $P < 0.05$. Tumor mutation burden (TMB), DNA mismatch repair (MMR), and microsatellite instability (MSI) have been demonstrated to correlate with the anti-tumor immune response in TME and influence the effectiveness of cancer immunotherapy [31-33]. Based on somatic mutation data and MMR gene expression levels obtained from TCGA, we analyzed the potential association of RBM34 with these three indicators in pan-cancer. Subsequently, we performed the Spearman correlation test to investigate the relationship between RBM34 expression and tumor stemness in different cancer types by extracting the RNA stemness scores (RNAss) or DNA methylation stemness scores (DNAss). Due to the lack of osteosarcoma data in the TISIDB database, we examined the correlation between RBM34 expression and human leukocyte antigen (HLA) genes and immune checkpoint genes (ICGs) with reference to previous studies [34]. In addition, we evaluated the half-maximal inhibitory concentration (IC50) of several targeted agents using information from the Cancer Genome Project (CGP) database (<http://www.sanger.ac.uk/genetics/CGP/>) to predict drug susceptibility in diverse RBM34-expressing osteosarcoma populations.

Functional enrichment analysis

The functional status of RBM34 in pan-cancer was examined at the single-cell level utilizing

RBM34 as a potential biomarker for osteosarcoma

the CancerSEA database (<http://biocc.hrbmu.edu.cn/CancerSEA/>) [35]. This investigation involved screening with p -values < 0.05 and correlation strength > 0.3 . In order to explore potential biological processes associated with osteosarcoma, the meta-cohort was divided into two subgroups based on the median level of RBM34 expression. Subsequently, the “limma” package was applied to determine differentially expressed genes (DEGs) between these subgroups, with an adjusted p -value < 0.05 . Following this, gene ontology (GO) and Kyoto Encyclopedia of Genes and Genomes (KEGG) pathway analyses were performed via the “clusterProfiler” package to investigate the cellular and molecular functions of RBM34-related DEGs (RRDEGs). Gene set enrichment analysis (GSEA) was also undertaken to explore the variability of activated pathways between the two subpopulations.

RBM34-derived genomic features

The entire osteosarcoma meta-cohort was randomized 1:1 into test and validation groups using the “caret” package, with the training cohort used to construct RBM34-derived genomic prognostic features and the test and total cohorts used to validate predictive performance. The interaction of RRDEGs with osteosarcoma prognosis was assessed using univariate Cox regression analysis with a p -value < 0.05 . Selected prognosis-associated RRDEGs were entered into least absolute shrinkage and selection operator (LASSO) and multivariate Cox regression analyses for further screening to develop an RBM34-derived prognostic index (RDPI). Based on gene expression levels (Expi) and correlation coefficients (Coefi), the RDPI score was calculated for individual osteosarcoma patients as follows: RDPI score = (Coefi \times Expi). Patients were subsequently categorized into high- and low-RDPI score subgroups based on the median RDPI score. Kaplan-Meier (KM) survival curves and receiver operating characteristic (ROC) curves were then plotted to assess the OS time of patients and the accuracy of the prognostic index, with simultaneous validation by the entire meta-cohort and validation group. Tumor purity and abundance of stromal and immune cells were calculated using the “ESTIMATE” package to assess discrepancies in the TME of patients with high and low RDPI scores.

Cell culture and quantitative real-time polymerase chain reaction (qRT-PCR)

Two osteosarcoma cell lines (MG-63, MNNG/HOS) were obtained through the Cell Bank of the Chinese Academy of Sciences (Shanghai, China) and cultured according to the instructions. Two RBM34 small interfering RNAs (siRNA) were purchased from GenePharma (Suzhou, China) and used to infect osteosarcoma cells according to the manufacturer’s protocol. Total RNA was prepared using RNAeasy™ isolation reagent (Vazyme Biotech Co., Ltd., Nanjing, China) and then reverse transcribed into cDNA with HiScript III RT SuperMix (Vazyme, China). Finally, qRT-PCR was performed using the UltraSYBR Mixture Kit (CW-BIO, China). GAPDH was set as internal control and relative gene expression was calculated by the $2^{-\Delta\Delta Ct}$ method. The primers for related genes and siRNA sequences for RBM34 knock-down are shown in [Supplementary Table 2](#).

Cell proliferation assay and transwell assay

Cell viability was assessed by a colony formation assay in which 1×10^3 osteosarcoma cells were inoculated in 6-well plates and cultured for 12 days before staining with crystal violet. For the CCK-8 assay, cells were seeded at a density of 1×10^3 cells/well in 96-well plates. Ten μ l of CCK-8 reagent was added at specific time points. After incubation at 37°C for one hour, optical density (OD) was measured at 450 nm. Transwell assays were conducted to analyze the effect of RBM34 on osteosarcoma cell migration and invasion. In the upper chamber, osteosarcoma cells were inoculated at 5×10^4 /well into serum-free medium, and in the lower chamber, 500 μ l of medium containing 10% FBS was added. Cells were seeded into the upper chamber with precoated Matrigel for invasion. After 24 hours, cells in the bottom chamber were fixed, stained, and photographed.

Flow cytometry and cell cycle analysis

The treated cells were collected and washed with PBS three times and fixed with iced 70% ethanol at 4°C overnight. After ethanol removal, cells were rinsed with ice-cold PBS and then treated with propidium iodide (PI) and RNase provided in the Cell Cycle Kit (BD Pharmingen, USA) for 15 min in the dark. The ratio of the cell

RBM34 as a potential biomarker for osteosarcoma

cycle phase was measured by the BD FACS Canto II (BD Biosciences, USA).

Western blotting

The collected cells were lysed with an appropriate volume of RIPA on ice for 30 min. The protein concentration was determined using the BCA protein assay kit (Thermo Fisher, USA). Protein blotting was performed by the SDS-PAGE electrophoresis system, and the PVDF membranes were incubated with the indicated primary and secondary antibodies. Then the signals were detected by enhanced chemiluminescence reagents (Vazyme, China). The antibodies used in this study were anti-RBM34 (A10139, 1:1000, ABclonal, Wuhan, China), anti-GAPDH (60004-1-Ig, 1:200000, Proteintech, Wuhan, China), HRP-conjugated affinipure goat anti-rabbit (SA00001-2, 1:6000, Proteintech, Wuhan, China) and anti-mouse (SA00001-1, 1:6000, Proteintech, Wuhan, China) IgG.

Statistical analysis

This study was based on R software (version 4.2.1) and GraphPad Prism 8.0 to analyze the data and generate graphs. All experiments were performed at least three times independently. Continuous variables were expressed using the mean \pm standard deviation. Statistical differences between groups were calculated by t-test or one-way ANOVA. $P < 0.05$ was considered statistically significant.

Results

Expression pattern of RBM34 in cancer cell lines, pan-cancer and osteosarcoma

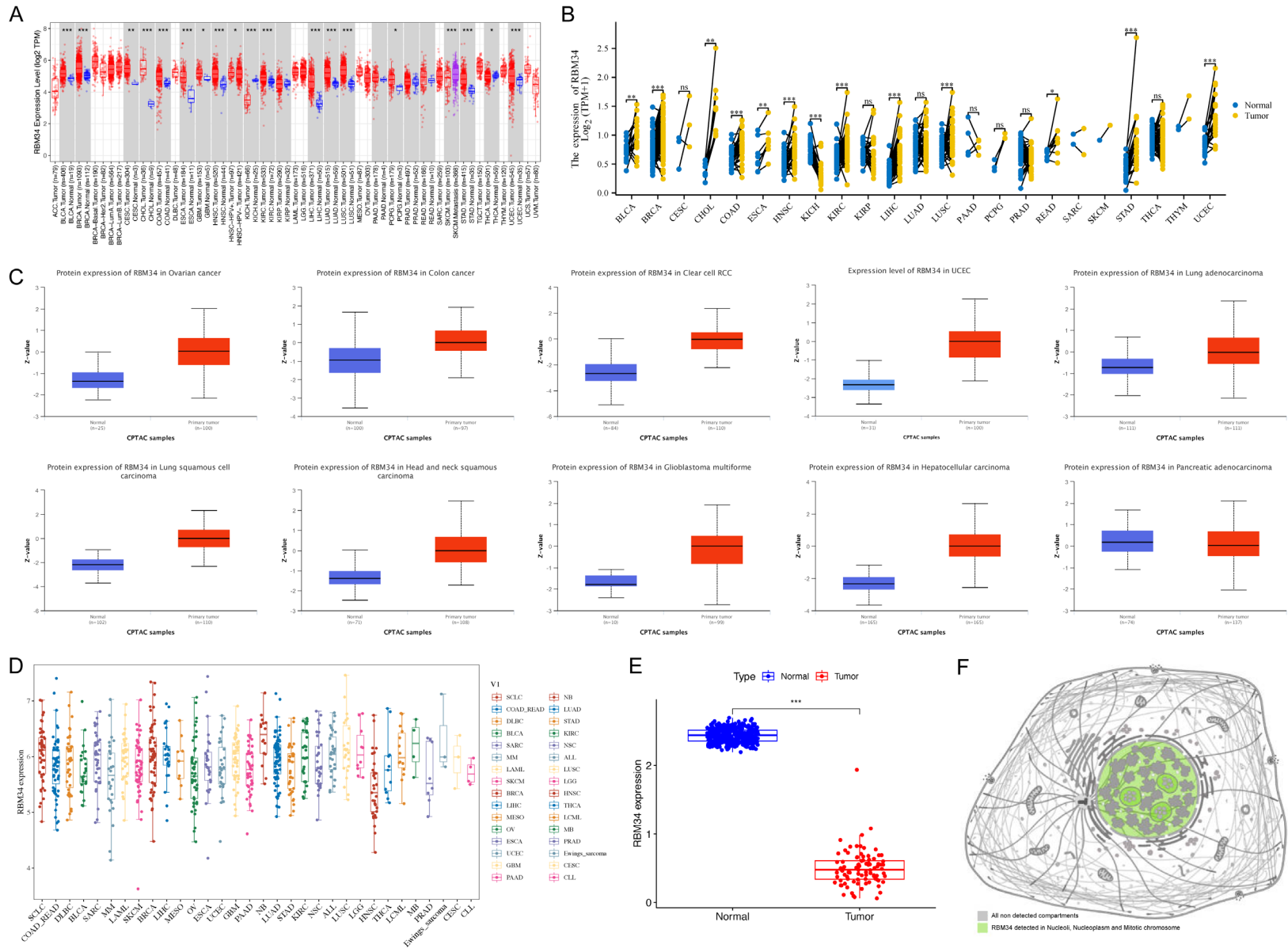
Based on the TIMER database, we investigated the expression abundance of RBM34 in pan-cancer. As shown in **Figure 1A**, RBM34 expression was significantly upregulated in 15 tumors compared to normal samples, including BLCA, BRCA, CESC, CHOL, COAD, ESCA, GBM, HNSC, KIRC, LIHC, LUAD, LUSC, PCPG, STAD, and UCEC. On the contrary, RBM34 mRNA levels were lower in KICH and THCA than in normal tissues (**Figure 1A**). Notably, the abundance of RBM34 was significantly elevated in HPV-positive HNSC and metastatic SKCM patients (**Figure 1A**). RNA-Seq analysis of TCGA showed that RBM34 was differentially expressed in 13 cancer types (BLCA, BRCA, CHOL, COAD, ESCA,

HNSC, KICH, KIRC, LIHC, LUSC, READ, STAD, and UCEC) compared to paired normal samples (**Figure 1B**). Furthermore, the UALCAN assessment revealed a significant elevation of RBM34 protein expression in nine human cancers, including OV, COAD, KIRC, UCEC, LUAD, LUSC, HNSC, GBM, and LIHC, while PAAD exhibited contrasting results (**Figure 1C**). The CCLE database provided relative expression levels of RBM34 in 32 tumor cell lines, indicating high expression in all cancer cell lines (**Figure 1D**). Integrating TARGET and GTEx data, we discovered that RBM34 mRNA expression was lower in osteosarcoma compared to non-tumor tissues (**Figure 1E**). Subsequently, the HPA database was utilized to examine the subcellular localization of RBM34, which demonstrated its distribution in the nucleoli, additionally to localization in the nucleoplasm and mitotic chromosome, potentially providing a physical basis for its involvement in RNA binding and selective splicing (**Figure 1F**). Further immunofluorescence localization of RBM34, nucleus, microtubules, and endoplasmic reticulum (ER) in U-2OS suggested that RBM34 was predominantly localized to nucleoli (**Figure 1G**).

Clinical correlation analysis and prognostic value of RBM34 in pan-cancer and osteosarcoma

KM plotter was employed to confirm the correlation between RBM34 expression and the prognosis of various cancers. Specifically, high RBM34 expression was unfavorable for OS in ACC ($P = 0.003$) and KIRC ($P = 0.004$) (**Figure 2A**). Meanwhile, patients with high RBM34 expression had poorer DSS in ACC ($P = 0.003$), UCEC ($P = 0.010$), and KIRC ($P = 0.023$) (**Figure 2B**). In contrast, LGG ($P = 0.026$) patients with high RBM34 expression exhibited significantly superior DSS (**Figure 2B**). There were disparities in DFI between patients with high and low RBM34 expression in six tumors, namely ACC, CESC, LUAD, READ, STAD, and UCEC ($P < 0.05$, **Figure 2C**). Upregulated RBM34 expression was associated with shorter PFI in ACC ($P < 0.001$), PRAD ($P = 0.034$), and UCEC ($P = 0.022$), but corresponded to longer PFI in LGG ($P = 0.006$) (**Figure 2D**). Furthermore, an examination was conducted to investigate the correlation between the expression of RBM34 and the pathological stage of various cancers. The analysis of our data demonstrated that the

RBM34 as a potential biomarker for osteosarcoma



RBM34 as a potential biomarker for osteosarcoma

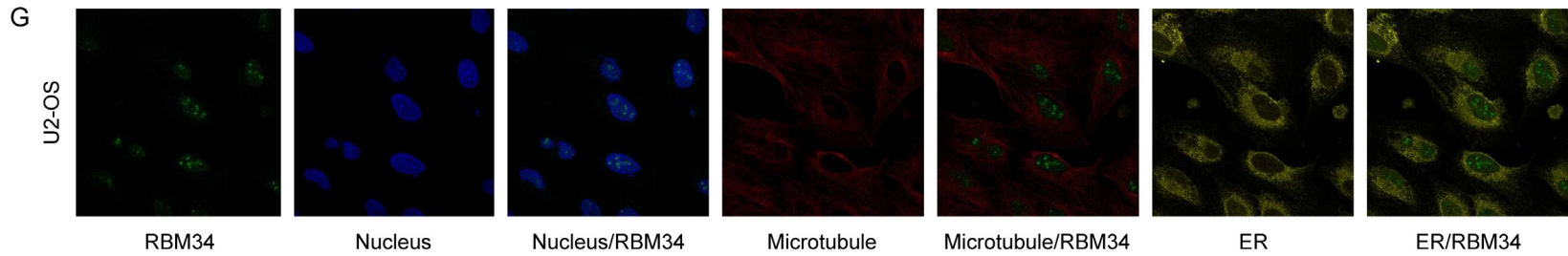
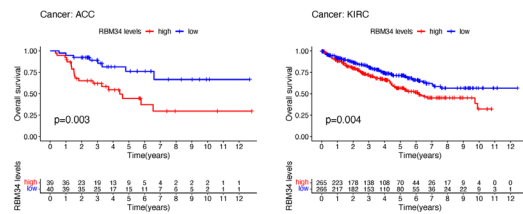
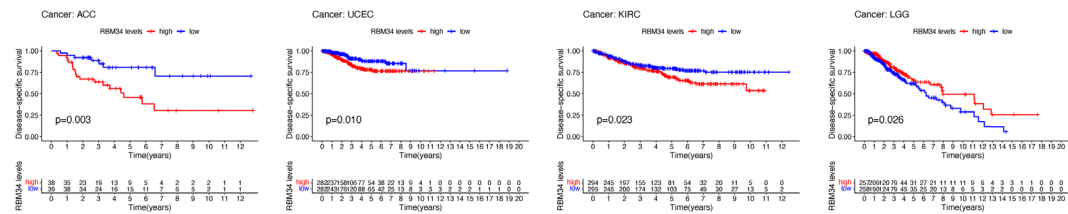


Figure 1. Expression pattern and subcellular localization of RBM34 from different databases. A. RBM34 mRNA expression in pan-cancer inferred by TIMER. B. RBM34 mRNA expression in TCGA cancer tissues compared to paired normal samples. C. RBM34 protein expression in multiple cancer types from the UALCAN database. D. RBM34 expression in tumor cell lines from the CCLE database. E. Comparison of RBM34 mRNA expression between osteosarcoma and normal samples. F. Subcellular localization of RBM34 in the HPA database. G. Immunofluorescence staining to detect subcellular localization of RBM34 in osteosarcoma.

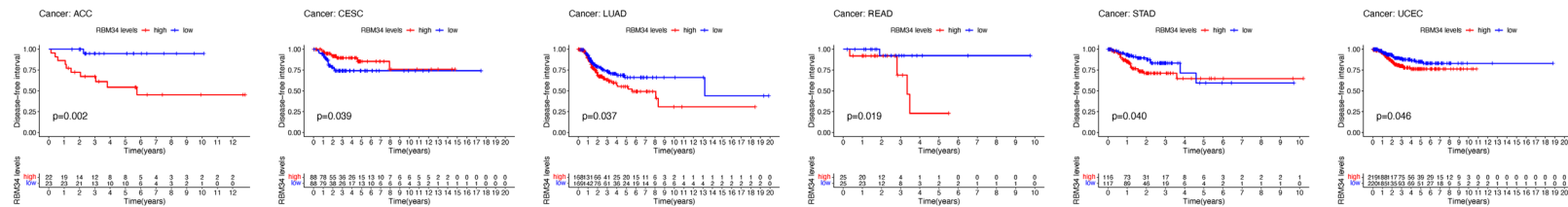
A Kaplan–Meier survival analysis (OS)



B Kaplan–Meier survival analysis (DSS)



C Kaplan–Meier survival analysis (DFI)



RBM34 as a potential biomarker for osteosarcoma

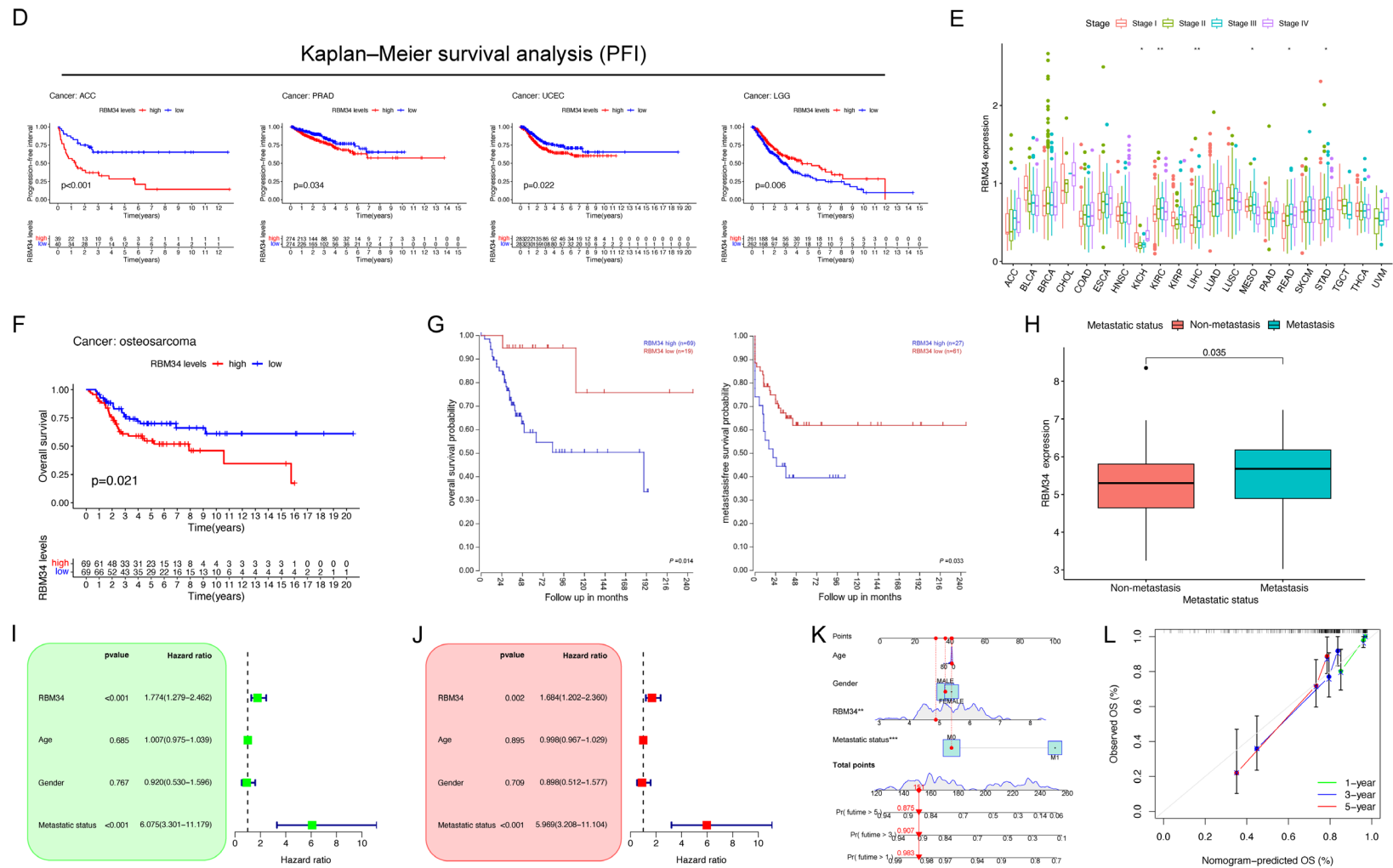


Figure 2. Prognostic analysis and clinical correlation analysis of RBM34. (A–D) Kaplan–Meier analysis of the association between RBM34 expression and overall survival (A), disease-specific survival (B), disease-free interval (C), and progression-free interval (D) in pan-cancer. (E) Associations between RBM34 expression and cancer stage in pan-cancer. (F) The impact of RBM34 on overall survival in osteosarcoma meta-cohort. (G) Survival analysis of RBM34 in the R2 database. (H) Associations between RBM34 expression and metastasis status in osteosarcoma. (I, J) Univariate (I) and multivariate (J) independent prognostic analysis of RBM34 and clinical variables. (K) Construction of an RBM34-based nomogram combining various clinicopathological parameters. (L) Calibration curve of the RBM34-based nomogram.

RBM34 as a potential biomarker for osteosarcoma

expression of RBM34 exhibited variations across different pathological stages in six types of tumors, namely KICH, KIRC, LIHC, MESO, STAD, and READ (**Figure 2E**). Specifically, in KICH and LIHC, the expression of RBM34 was higher in stage IV compared to stages I, II, and III (**Figure 2E**). However, the opposite trend was observed in MESO and STAD, where RBM34 expression was lower in stage IV (**Figure 2E**).

Additionally, the investigation of osteosarcoma meta-cohort indicated that patients with high RBM34 expression had shorter OS times (**Figure 2F**). Similarly, increased RBM34 expression is accompanied by reduced OS and metastasis-free survival in osteosarcoma, as indicated by the R2 database (**Figure 2G**). Clinical correlation analysis revealed that the expression of RBM34 was significantly elevated in cases of metastatic osteosarcoma compared to localized osteosarcoma (**Figure 2H**). Univariate and multivariate Cox regression analyses were employed to examine the association between RBM34 expression and clinical factors (age, gender, and metastasis status) with OS in osteosarcoma. The findings demonstrated that metastasis status and RBM34 were independent prognostic elements in osteosarcoma patients with p -values < 0.05 (**Figure 2I, 2J**). We then created a nomogram combining RBM34 and clinicopathological variables for osteosarcoma patients to facilitate the convenient prediction of OS at 1, 3, and 5 years (**Figure 2K**). The conformity between the predicted and actual OS probabilities was assessed by calibration curves (**Figure 2L**).

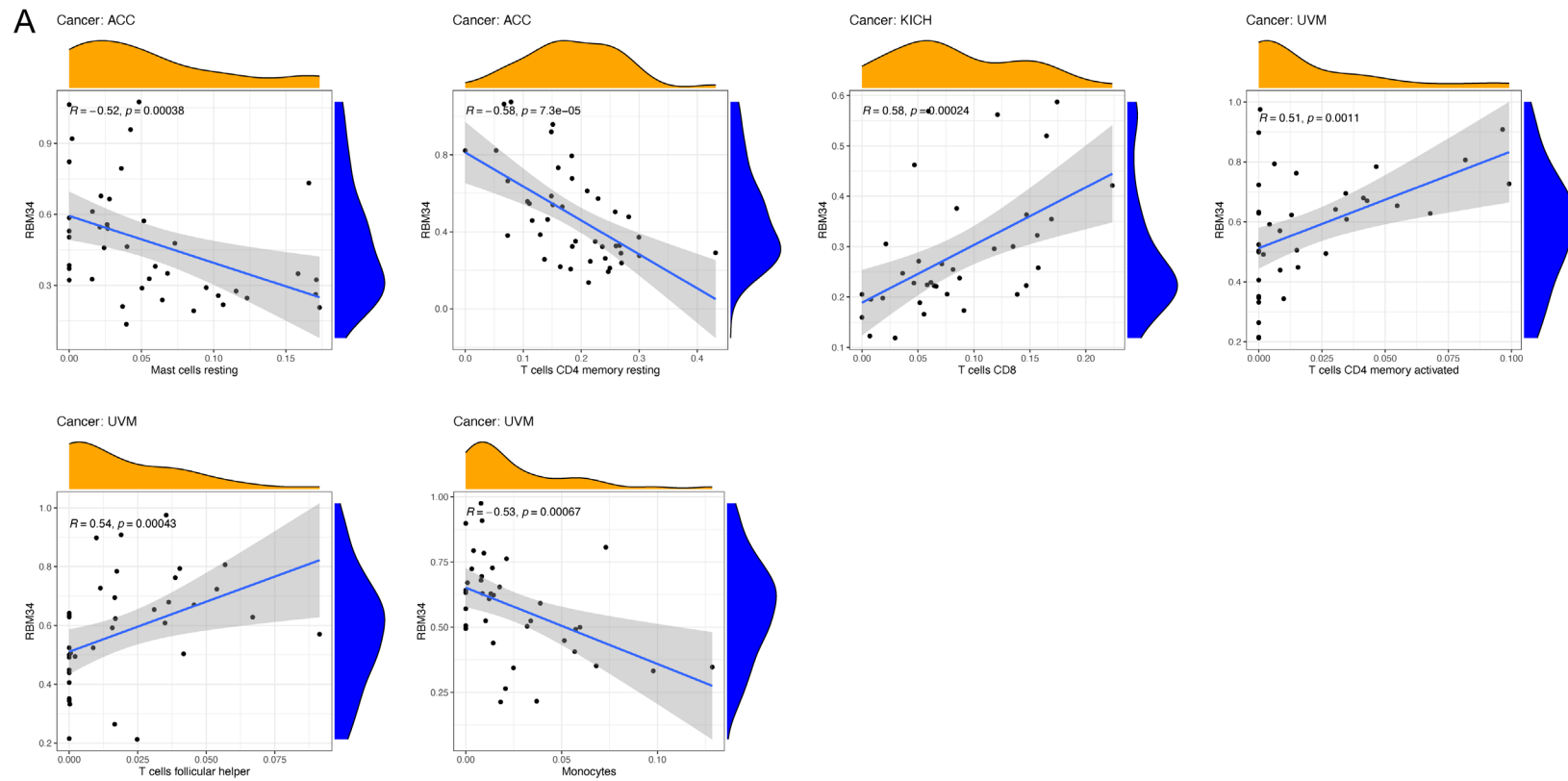
The pertinence of RBM34 with TME and immunological features in pan-cancer

The establishment of an immunosuppressive microenvironment plays a crucial role in the progression of tumors. In order to explore the potential association between RBM34 expression and the immune landscape, we conducted a comprehensive investigation utilizing the TISIDB database, as well as the ESTIMATE and CIBERSORT algorithms. By employing the CIBERSORT algorithm, we observed that in ACC, RBM34 expression exhibited a negative correlation with resting mast cells and resting memory CD4⁺ T cells (**Figure 3A**). Conversely, in KICH, RBM34 expression demonstrated a positive correlation with CD8⁺ T cells (**Figure**

3A). Furthermore, in UVM, RBM34 expression displayed a positive correlation with activated memory CD4⁺ T cells and follicular helper T cells, and a negative correlation with monocytes (**Figure 3A**). **Figure 3B** indicates a robust association between the ESTIMATE score and RBM34 expression. In CHOL and LGG, stromal scores exhibited a negative correlation with RBM34 expression (**Figure 3B**). On the other hand, KICH and THYM exhibited a positive correlation between RBM34 expression and immune score (**Figure 3B**). Moreover, in DLBC, RBM34 expression was negatively related to ESTIMATE Score, while in KICH, it was positively associated with ESTIMATE Score, but conversely for tumor purity (**Figure 3B**).

Immunomodulators and chemokines play a crucial role in influencing the functionality of the immune system. To further investigate this relationship, we examined the association between RBM34 expression and various factors such as TILs, immunomodulators, chemokines, and receptors in pan-cancer utilizing the TISIDB database. **Figure 4A** illustrates the correlation between RBM34 and 28 immune cell subtypes across 30 tumors. Significantly, within the context of ACC, RBM34 expression demonstrated a notably robust positive correlation with $\gamma\delta$ T cells ($\rho = 0.517$, $P < 0.001$, **Figure 4A**). Conversely, in UVM, RBM34 expression exhibited a pronounced negative correlation with monocytes ($\rho = -0.632$, $P < 0.001$, **Figure 4A**). Among the 45 immunostimulators examined, RBM34 expression in CHOL displayed the most substantial positive correlation with TNFSF14 ($\rho = 0.518$, $P < 0.01$); while in TGCT, it demonstrated the strongest negative correlation with TNFSF15 ($\rho = -0.561$, $P < 0.001$, **Figure 4B**). Regarding immunoinhibitors, RBM34 expression in ACC exhibited the most prominent positive correlation with IL10RB ($\rho = 0.568$, $P < 0.001$), whereas, in UVM, it displayed the strongest negative correlation with PVRL2 ($\rho = -0.545$, $P < 0.001$, **Figure 4C**). In the context of 41 chemokines, RBM34 expression exhibited the most robust positive correlation with CXCL2 in CHOL ($\rho = 0.353$, $P < 0.05$); while in READ, it demonstrated the strongest negative correlation with CCL23 ($\rho = -0.61$, $P < 0.001$, **Figure 4D**). Among 18 chemokine receptors, RBM34 expression displayed the highest positive correlation with CXCR3 in TGCT ($\rho = 0.283$, $P <$

RBM34 as a potential biomarker for osteosarcoma



RBM34 as a potential biomarker for osteosarcoma

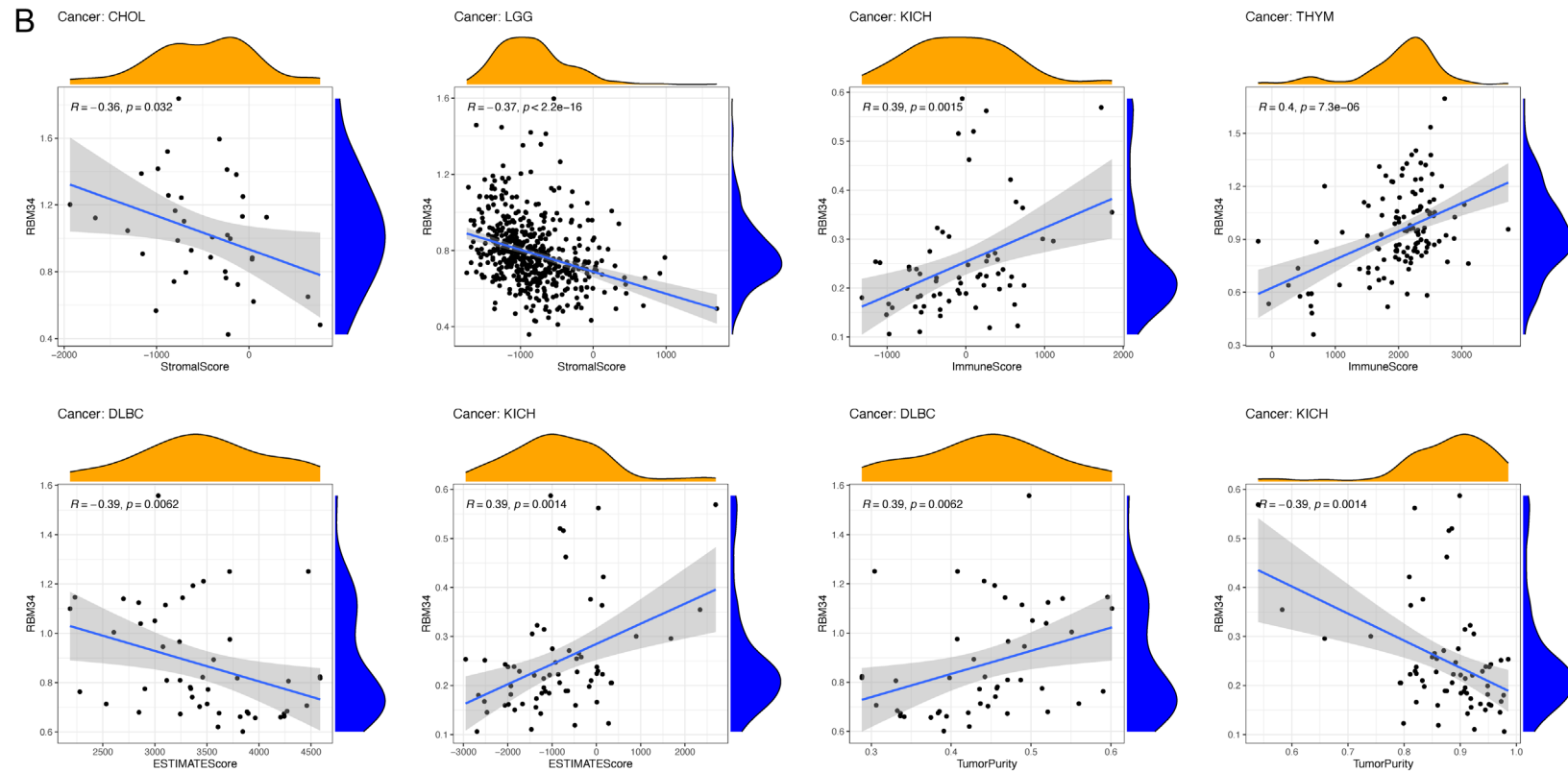


Figure 3. The pertinence of RBM34 with tumor microenvironment using ESTIMATE and CIBERSORT algorithms. A. Correlation of RBM34 with tumor-infiltrating lymphocytes in pan-cancer. B. Correlation between RBM34 and ESTIMATE analysis in pan-cancer.

0.001); whereas, in READ, it exhibited the strongest negative correlation with CCR10 ($\rho = -0.594$, $P < 0.001$, **Figure 4E**). Regarding the 21 MHC molecules, RBM34 expression exhibited the most significant positive correlation with TAPBP in PCPG ($\rho = 0.38$, $P < 0.001$); while in READ, it displayed the strongest negative correlation with HLA-G ($\rho = -0.561$, $P < 0.001$, **Figure 4F**).

Association of RBM34 with pan-cancer immune response

TMB, MSI, and MMR are recognized as biomarkers for predicting the effectiveness of immunotherapy. High TMB levels correlated with increased levels of RBM34 among patients with certain cancers such as BRCA, ACC, SKCM, READ, PAAD, LGG, HNSC, and COAD, while in UCS, THYM, and SARC, RBM34 was negatively associated with TMB (**Figure 5A**). The distribution of MSI among patients is depicted in **Figure 5B**. Notably, the correlation between MSI and RBM34 expression was positive in 11 tumors (UCEC, THCA, STAD, READ, LUAD, LUSC, HNSC, DLBC, COAD, BRCA, and BLCA) and negative in 4 tumors (ACC, SARC, CESC, and KIRC) (**Figure 5B**). Subsequently, we conducted an investigation into the co-expression of RBM34 and MMR genes, including MLH1, MSH2, MSH6, PMS2, and EPCAM. Our findings revealed a positive correlation between RBM34 and MSH2 in the majority of cancer types, with the most pronounced positive correlation observed in KICH (**Figure 5C**). Additionally, RBM34 demonstrated a significant association with all MMR-related genes in BRCA, LGG, and THCA (**Figure 5C**). Cancer stemness assessments highlighted RBM34 with varying degrees of association with RNAss and DNAss in different cancer types (**Figure 5D**). It was positively affiliated with RNAss in 16 cancers (including ACC, BLCA, BRCA, CESC, CHOL, GBM, HNSC, LAML, LGG, LIHC, LUSC, MESO, PAAD, PCPG, SARC, and THYM), but highly negatively related to DNAss in THYM (**Figure 5D**).

Immune and pharmacogenomic characterization of RBM34 in osteosarcoma

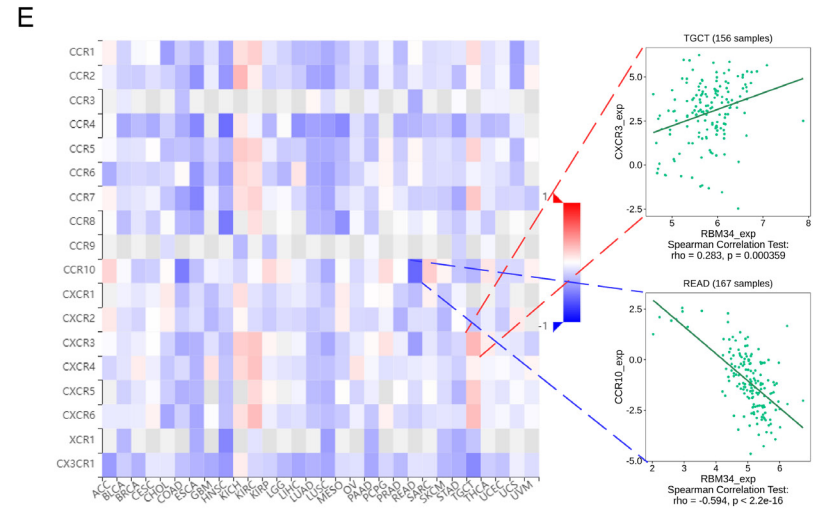
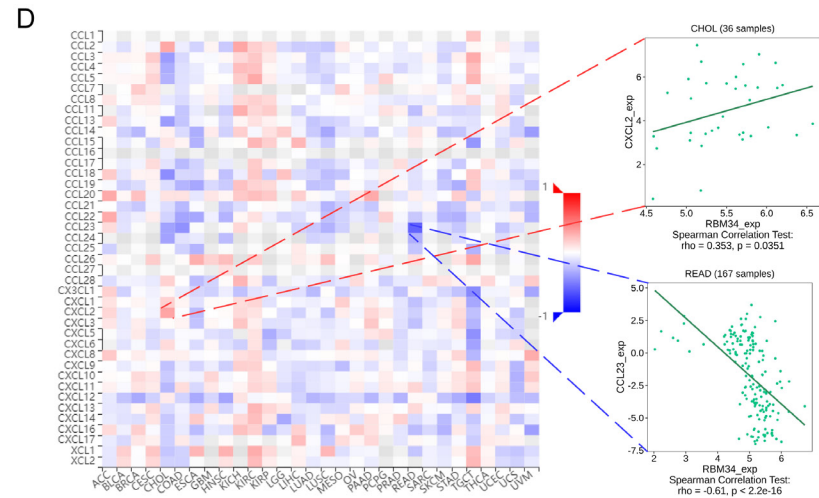
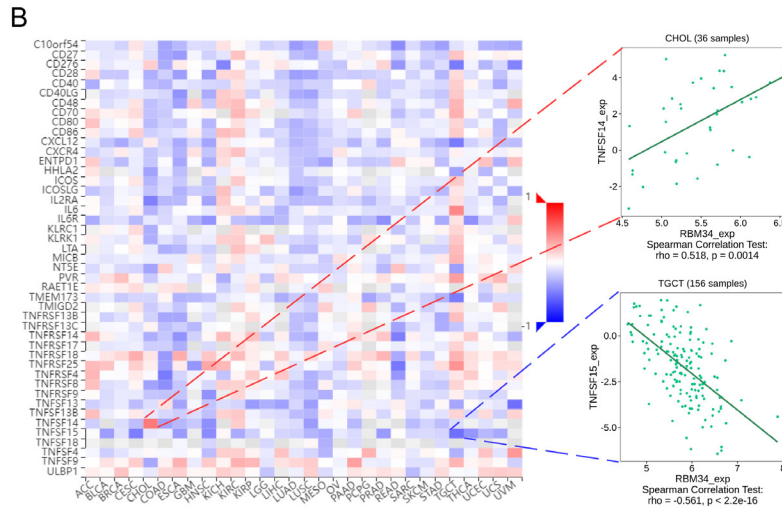
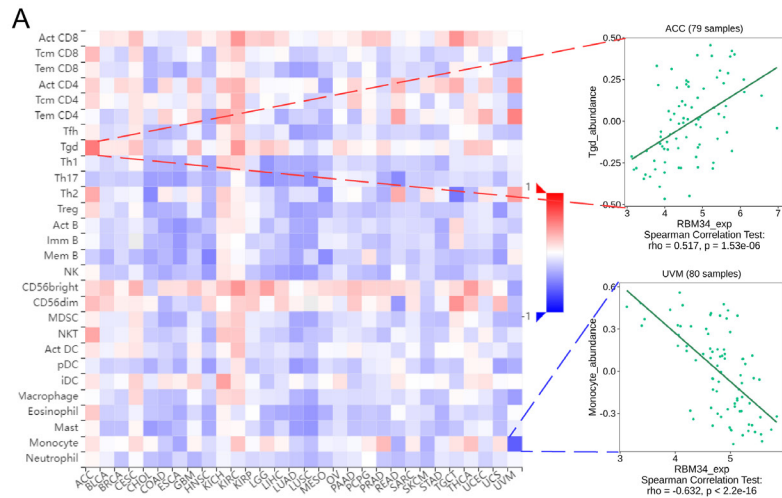
In the ESTIMATE analysis of osteosarcoma patients, RBM34 expression exhibited a negative correlation with ESTIMATE and stromal scores but a positive correlation with tumor purity (**Figure 6A**). The CIBERSORT algorithm

was used to investigate the correlation between RBM34 and the degree of immune cell infiltration. The results indicated a positive correlation between RBM34 expression and the infiltration level of resting memory CD4+ T cells and activated NK cells (**Figure 6B**). In contrast, RBM34 expression was negatively correlated with $\gamma\delta$ T cell abundance in osteosarcoma (**Figure 6B**). To deepen the understanding of the immunotherapeutic value of RBM34 in osteosarcoma, the co-expression relationship between RBM34 and ICGs and HLA genes was explored. **Figure 6C** demonstrates a significant association between RBM34 and various ICGs in osteosarcoma, including PD-1, PD-L1, CTLA4, TIGIT, LAG3, HAVCR2, and PDCD1LG2. Regarding universally confirmed HLA genes, high expression of RBM34 is linked to the upregulation of HLA-H, HLA-G, and HLA-C in osteosarcoma (**Figure 6D**). Additionally, there is a notable disparity in the IC50 values of 20 targeted drugs among osteosarcoma patients with diverse RBM34 expression. Specifically, higher RBM34 expression correlates with increased sensitivity to AICAR, Camptothecin, Cisplatin, and Mitomycin.C (**Figure 6E**). On the other hand, Bexarotene, BI.2536, Bicalutamide, CGP.60474, DMOG, FTI.277, GNF.2, GSK269-962A, JW.7.52.1, KIN001.135, Lapatinib, NVP. TAE684, PF.02341066, PHA.665752, Roscovitine, and Shikonin had lower IC50 values in the low RBM34 expression subgroup (**Figure 6E**).

Functional analysis of RBM34 in pan-cancer and osteosarcoma

We utilized CancerSEA to further investigate the molecular mechanisms of RBM34 in pan-cancer at the single-cell level (**Figure 7A**). There was a negative relationship between RBM34 and DNA repair, DNA damage, and apoptosis in UM (**Figure 7B**). However, there was a positive relationship between RBM34 and stemness in NSCLC (**Figure 7B**). In the context of LUAD, RBM34 expression demonstrated a particularly robust positive correlation with DNA repair, but the opposite for metastasis (**Figure 7B**). Moreover, RBM34 was negatively associated with invasion in AML, OV, and CRC, and with the cell cycle in ALL (**Figure 7B**). In RB, RBM34 was positively correlated with angiogenesis, differentiation, and inflammation, but negatively correlated with DNA repair, cell cycle, and DNA damage (**Figure 7B**).

RBM34 as a potential biomarker for osteosarcoma



RBM34 as a potential biomarker for osteosarcoma

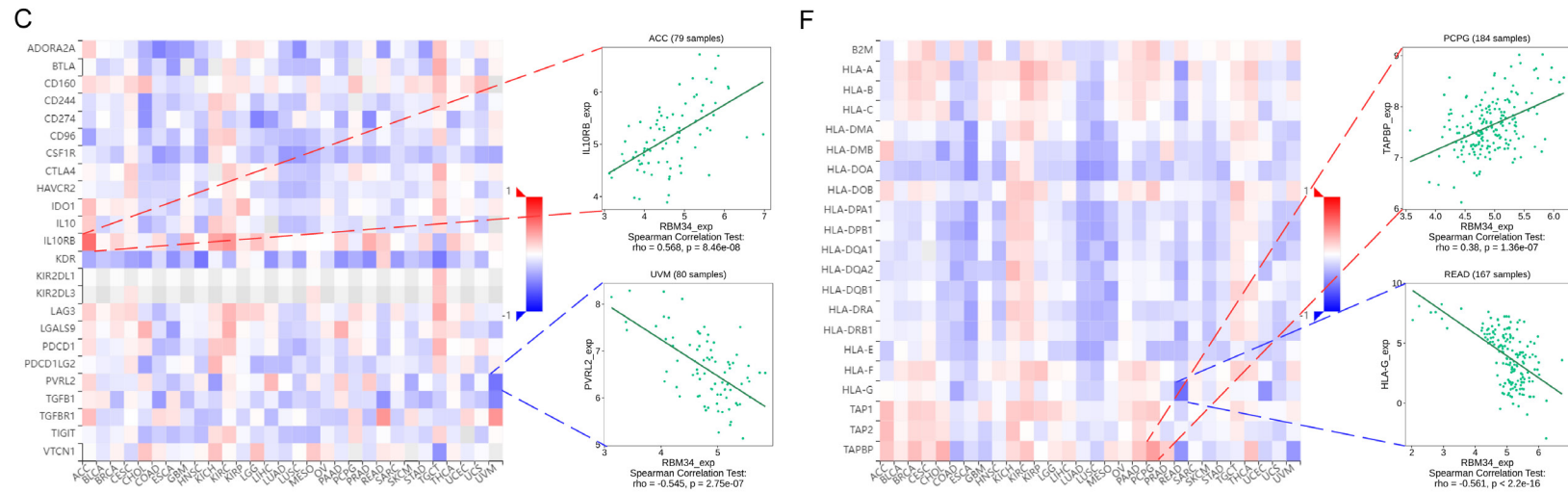


Figure 4. Investigation of the correlation between RBM34 and immunological characteristics utilizing the TISIDB database. A. Correlation of RBM34 with tumor-infiltrating lymphocytes in the TISIDB database. B. Correlation of RBM34 with immunostimulators in the TISIDB database. C. Correlation of RBM34 with immunoinhibitors in the TISIDB database. D. Correlation of RBM34 with chemokines in the TISIDB database. E. Correlation of RBM34 with chemokine receptors in the TISIDB database. F. Correlation of RBM34 with MHC molecules in the TISIDB database.

RBM34 as a potential biomarker for osteosarcoma

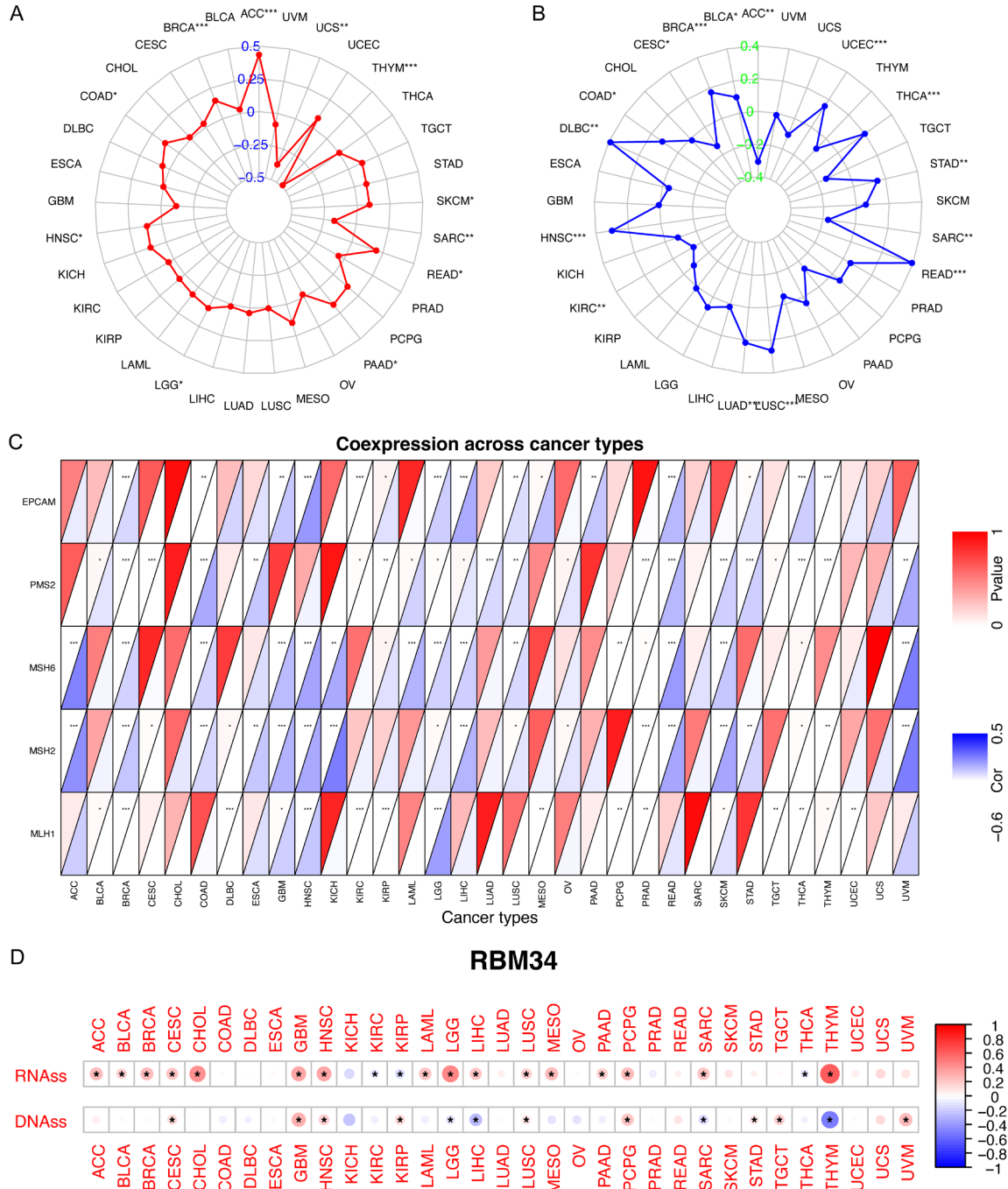
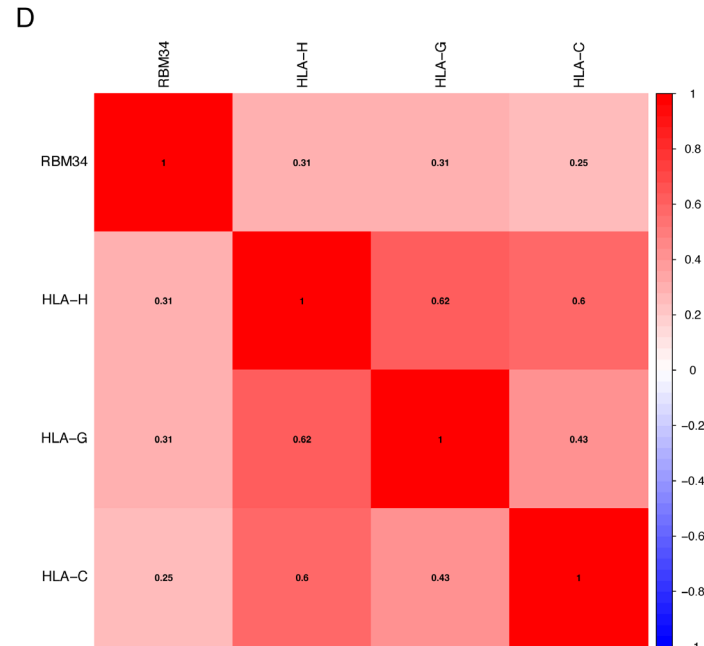
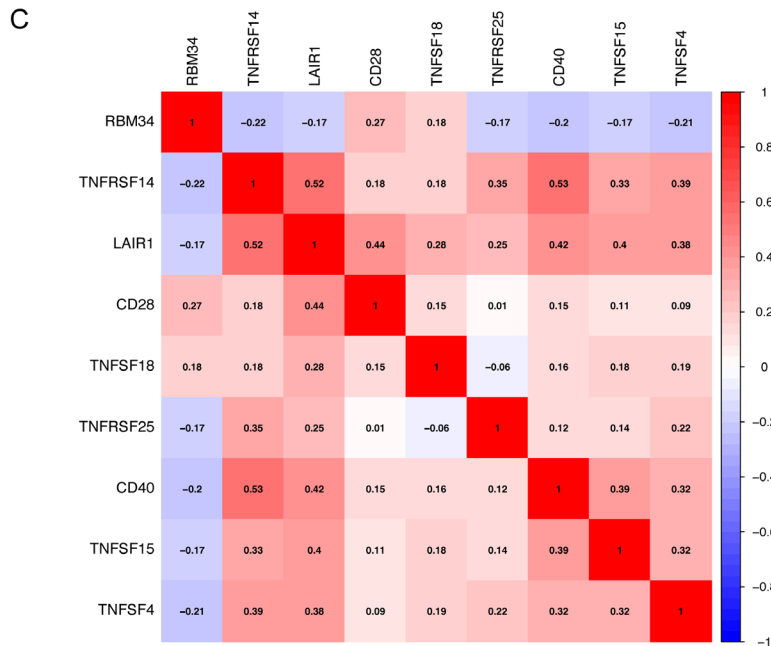
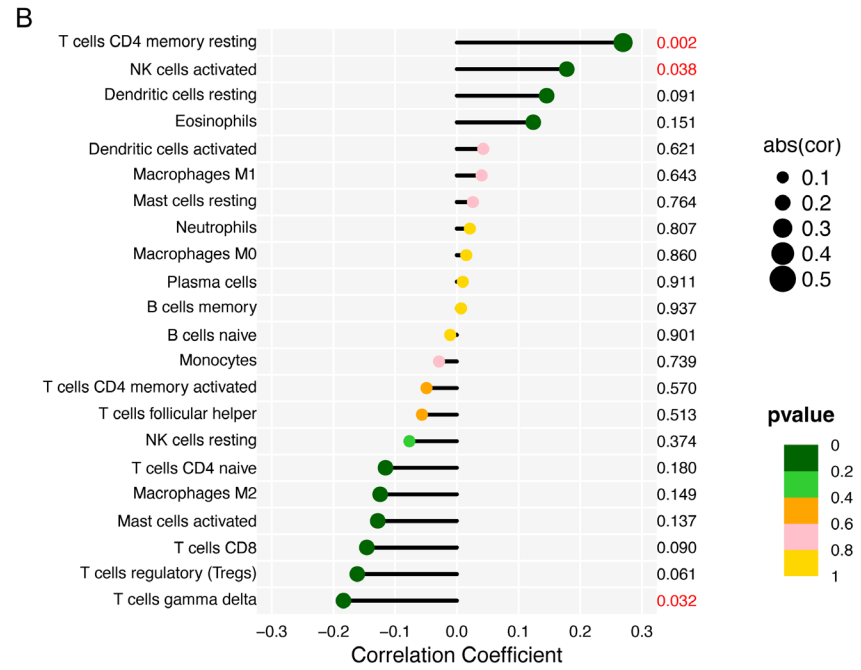
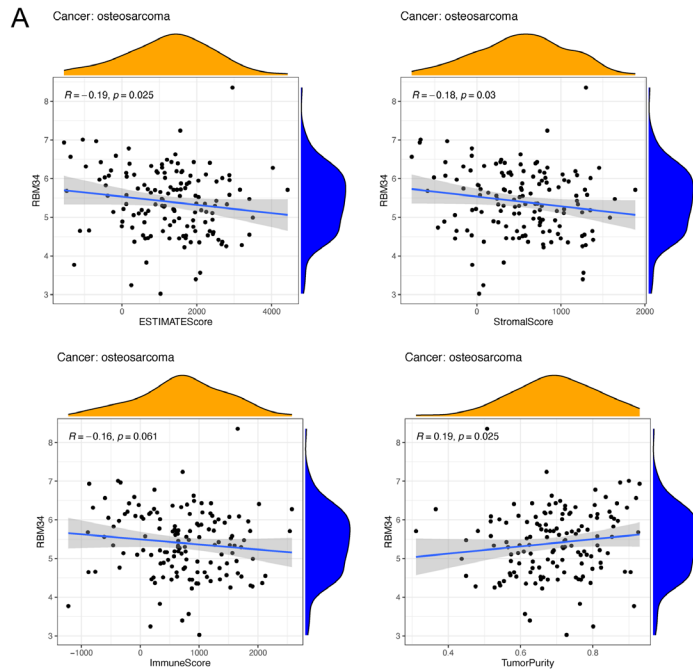


Figure 5. Correlation of RBM34 with immunotherapy response and cancer stemness in pan-cancer. A. Correlations of RBM34 with tumor mutation burden in pan-cancer. B. Correlations of RBM34 with microsatellite instability in pan-cancer. C. Correlations of RBM34 with DNA mismatch repair in pan-cancer. D. Correlations of RBM34 with cancer stemness in pan-cancer.

To investigate the potential role of RBM34 in osteosarcoma, we extracted DEGs between patients with high and low RBM34 expression for GO, KEGG, and GSEA enrichment analyses. The heatmap displays the top 50 up- or down-

regulated genes between distinct RBM34-expressing groups (Figure 7C). GO-BP enrichment analysis demonstrated that most of these RRDEGs are enriched in the histone modification, proteasome-mediated ubiquitin-depen-

RBM34 as a potential biomarker for osteosarcoma



RBM34 as a potential biomarker for osteosarcoma

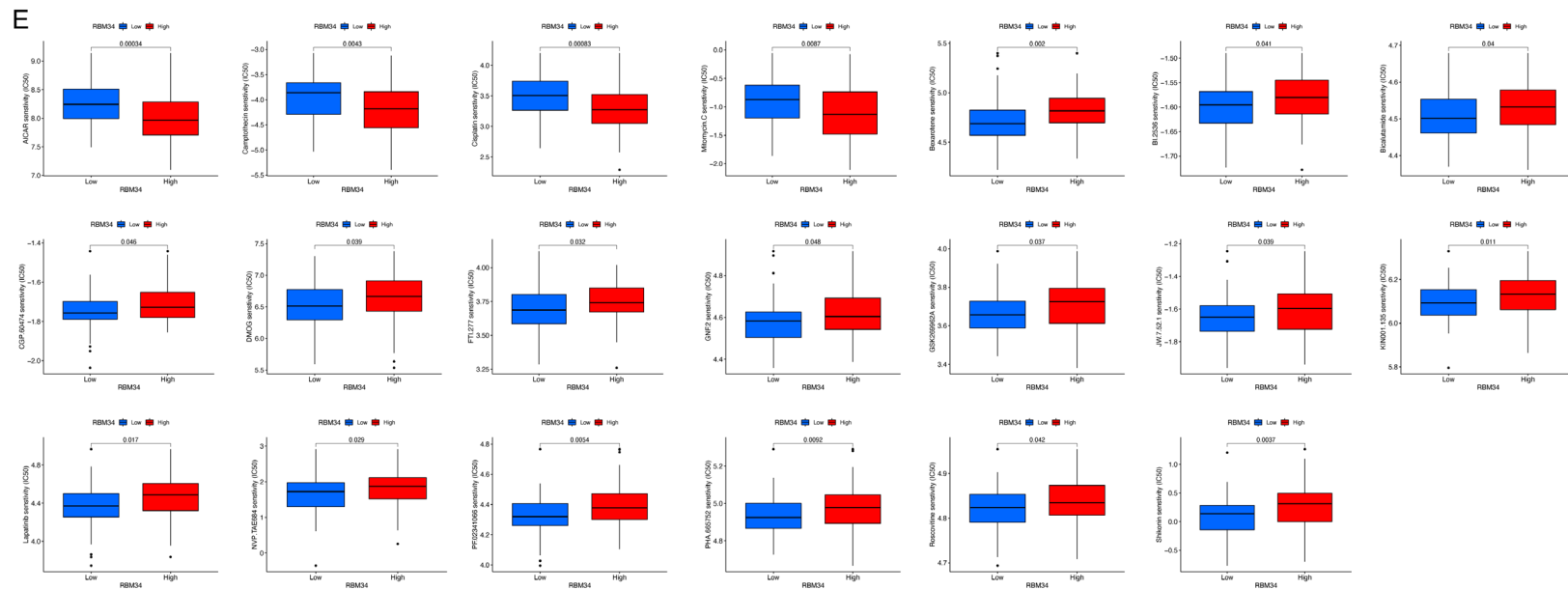


Figure 6. Immune correlation analysis and drug sensitivity analysis of RBM34 in osteosarcoma. A. ESTIMATE analysis of RBM34 in osteosarcoma. B. Connection of RBM34 expression with tumor-infiltrating immune cells in osteosarcoma. C. Correlations of RBM34 with immune checkpoint genes in osteosarcoma. D. Correlations of RBM34 with human leukocyte antigen genes in osteosarcoma. E. Discrepancies in drug sensitivity between diverse RBM34-expressing osteosarcoma populations.

RBM34 as a potential biomarker for osteosarcoma

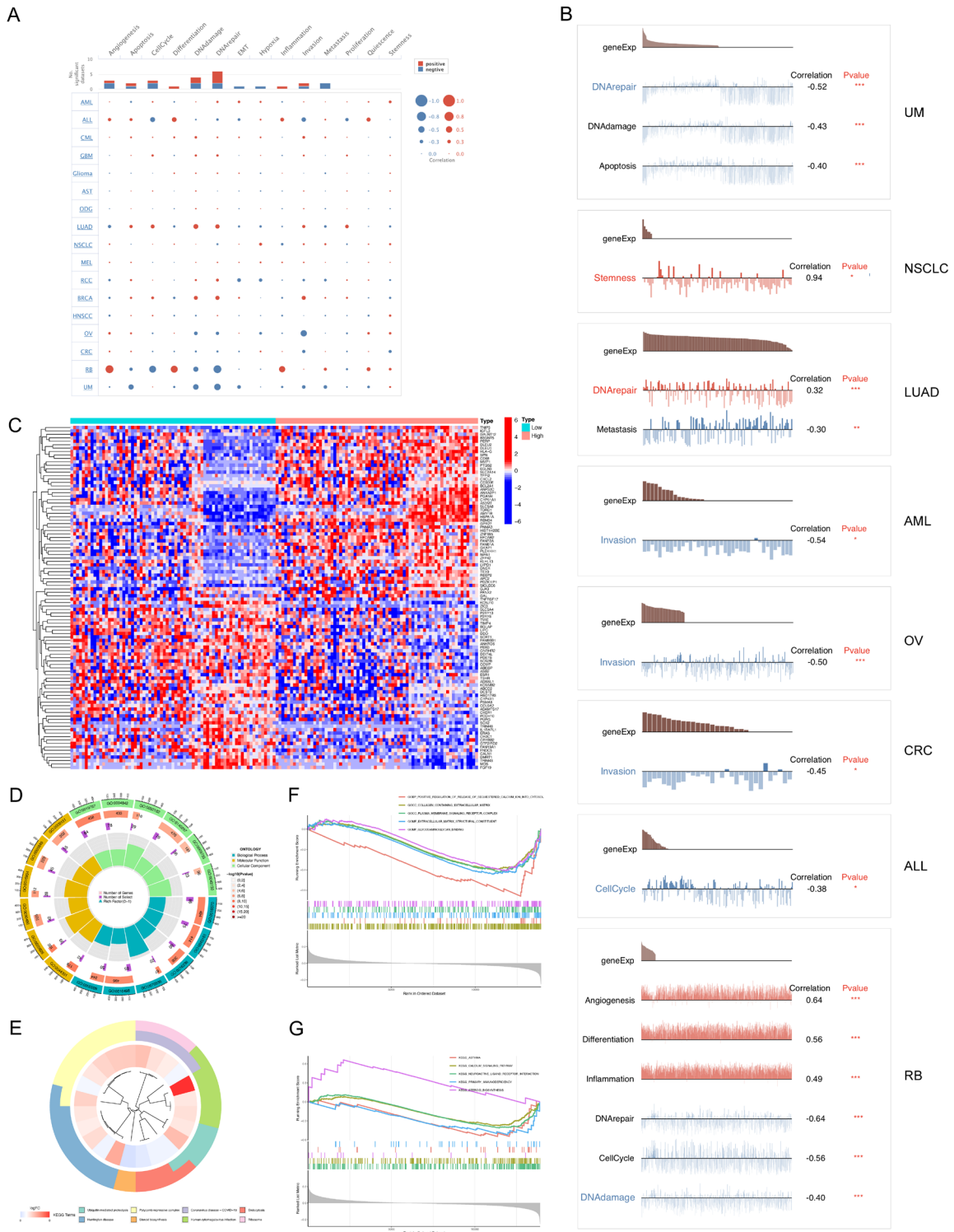


Figure 7. Functional Analysis of RBM34. (A) Single-Cell Functional Analysis of RBM34 from the CancerSEA database. (B) Functional status of RBM34 in various tumors. (C) Differentially expressed genes between high and low RBM34 expression groups. (D, E) GO (D) and KEGG (E) enrichment analyses of RBM34-related genes. (F, G) GSEA enriched functions (F) and pathways (G) in diverse RBM34-expressing osteosarcoma populations.

dent protein catabolic process, macroautophagy, and proteasomal protein catabolic process

(Figure 7D; Supplementary Table 3). As for CC and MF terms, RRDEGs were involved in ribo-

RBM34 as a potential biomarker for osteosarcoma

somal subunit, cytosolic ribosome, midbody, ubiquitin-like protein transferase activity, ubiquitin-protein transferase activity, and ubiquitin-like protein binding (**Figure 7D**; [Supplementary Table 3](#)). KEGG enrichment determined numerous underlying mechanisms related to ubiquitin-mediated proteolysis, polycomb repressive complex, and endocytosis (**Figure 7E**; [Supplementary Table 3](#)). As revealed by GESA analysis, five GO categories, including positive regulation of release of sequestered calcium ion into cytosol, collagen-containing extracellular matrix, plasma membrane signaling receptor complex, extracellular matrix structural constituent, and glycosaminoglycan binding were significantly activated in the RBM34 low-expression group (**Figure 7F**). **Figure 7G** illustrates that the steroid biosynthesis pathway was up-regulated and the neuroactive ligand-receptor interaction, primary immunodeficiency, calcium signaling pathway, and asthma pathways were down-regulated in the high expression group of RBM34.

Construction of an RBM34-derived genomic prognostic index for osteosarcoma

Univariate Cox analysis was first conducted to screen for RRDEGs that significantly influenced patient outcomes ([Supplementary Figure 1A](#)). The RBM34-derived prognostic index (RDPI) was subsequently developed for application to specific individuals by Lasso and multivariate Cox regression ([Supplementary Figure 1B, 1C](#)). The formula of RDPI is as follows: $\text{RDPI score} = (0.82168 \times \text{FAM81A}) + (-0.96743 \times \text{BBS4}) + (-4.71597 \times \text{FBXL5}) + (-2.23955 \times \text{LBR}) + (1.45352 \times \text{SYNGAP1}) + (-0.73151 \times \text{ZNF610})$. Each osteosarcoma sample from the train, validation, or entire cohort was calculated for the RDPI score and stratified into high- and low-RDPI scoring groups ([Supplementary Figure 1D-E](#)). As observed, FAM81A and SYNGAP1 were enriched in the high RDPI scoring group, while the opposite was true for BBS4 and FBXL5 ([Supplementary Figure 1D-E](#)). The PCA analysis revealed the heterogeneity and effective differentiation of patients across RDPI score groups ([Supplementary Figure 1G](#)). [Supplementary Figure 1H](#) illustrates that osteosarcoma patients with high RDPI scores had increased mortality compared to those with low RDPI scores in all three cohorts. The RDPI scoring system was highly accurate in the training cohort, with AUCs greater than 0.85 at

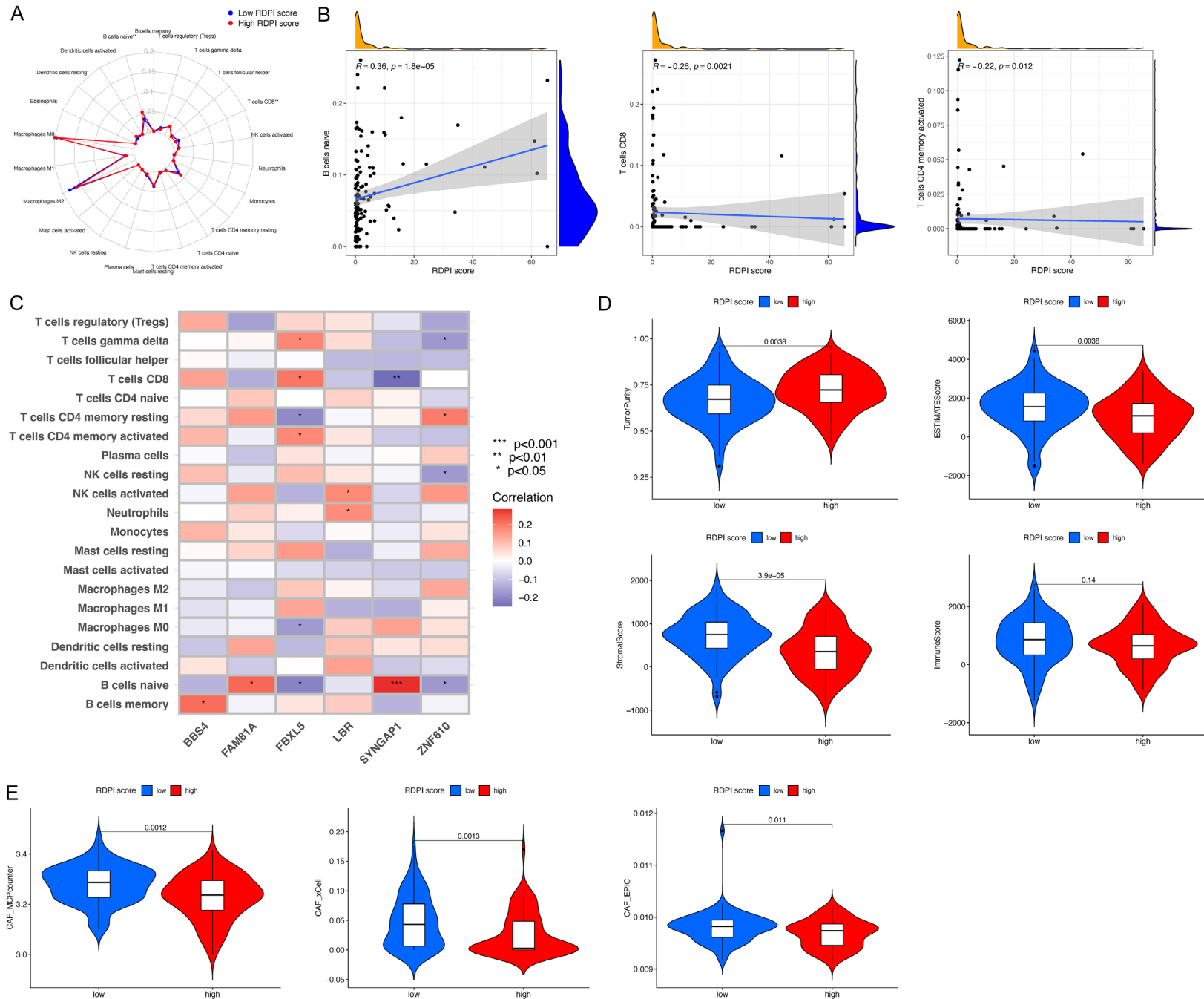
1, 3, and 5 years ([Supplementary Figure 1I](#)). ROC curve analysis conducted on the test or entire cohort consistently reflected that the RDPI was a reliable prognostic indicator for osteosarcoma, with AUCs greater than 0.7 at 1, 3, and 5 years ([Supplementary Figure 1I](#)).

For the immune landscape of distinct RDPI score groups, we uncovered significant variations in four cell types correlated with innate or adaptive immunity, including naive B cells, CD8+ T cells, resting dendritic cells, and activated CD4+ memory T cells (**Figure 8A**). Notably, RDPI scores were positively correlated with naive B cells, but negatively with CD8+ T cells and activated CD4+ memory T cells (**Figure 8B**). Among the six RRDEGs, FBXL5 was linked to the infiltration of six immune cells, including naive B cells, M0 Macrophages, activated CD4+ memory T cells, resting CD4+ memory T cells, CD8+ T cells, and $\gamma\delta$ T cells (**Figure 8C**). On the other hand, the expression of SYNGAP1 manifested a strong positive correlation with infiltrated naive B cells (**Figure 8C**). The ESTIMATE algorithm revealed significant differences in immunological subtypes between RDPI score groups, with increasing RDPI scores accompanying elevated tumor purity, but the reverse for ESTIMATE score and stromal score (**Figure 8D**). CAF is one of the major stromal cells in TME and is valuable in immune dysregulation, tumor diagnosis, and prognostic evaluation. By inferring the proportion of CAF in osteosarcoma patients by MCPCounter, xCELL, and EPIC algorithms, we found significant differences in the abundance of CAFs between the two RDPI score groups (**Figure 8E**). Cox regression was employed to appraise the independent prognostic value of RDPI scores, and the results declared that metastasis status and RDPI scores were independent prognostic elements in osteosarcoma patients ([Supplementary Figure 2A, 2B](#)). Furthermore, the clinicopathologic parameters of the two RDPI score groups were compared. There were no significant disparities in age as well as gender between the diverse RDPI score groups, but the probability of metastasis was higher in patients with high RDPI scores ([Supplementary Figure 2C-E](#)).

RBM34 promotes the proliferation and metastasis of osteosarcoma cells

In order to further investigate the role of RBM34 in osteosarcoma cells, we employed siRNA

RBM34 as a potential biomarker for osteosarcoma



RBM34 as a potential biomarker for osteosarcoma

Figure 8. Extended application of RDPI score in the immune landscape. A. Comparison of immune cell infiltration in diverse RDPI score subgroups. B. Correlation analysis between RDPI score and immune infiltrating cells. C. Correlation analysis between RRDEGs and immune infiltrating cells. D. ESTIMATE analysis of diverse RDPI score subgroups. E. Comparison of CAF proportion scores for diverse RDPI score subgroups with MCP-Counter, xCell, and EPIC algorithms. RRDEGs, RBM34-related differentially expressed genes; RDPI, RBM34-derived prognostic index.

transfection to downregulate the expression of RBM34. Both RBM34 mRNA and protein expression levels were markedly decreased in si-RBM34 MG-63 and MNNG/HOS cells compared to controls (**Figure 9A, 9B**). **Figure 9C, 9D** demonstrated that reducing RBM34 expression led to a decrease in the number of migrating and invading osteosarcoma cells. Furthermore, the proliferation abilities of si-RBM34 osteosarcoma cells were significantly inhibited as evidenced by CCK8 and clone formation assays (**Figure 9E, 9F**). The cell cycle distribution showed that RBM34 knockdown significantly increased the proportion of cells in the G1 phase (**Figure 9G**). This means that it induced the G0-G1 phase arrest, suggesting that RBM34 could regulate the cell cycle and impair cell proliferation.

Discussion

Osteosarcoma remains a global medical challenge with poor prognosis and high mortality [29]. Its pathogenesis is characterized by diverse and complex features, including karyotypic instability, genomic aberrations, and structural chromosomal abnormalities [36-38]. Late diagnosis, tumor metastasis, and rapid progression contribute to the high mortality rate of osteosarcoma patients, and current therapeutic strategies are suboptimal [39]. Therefore, it is necessary to further investigate the underlying pathogenesis of osteosarcoma from new perspectives and to seek effective systemic therapies to improve the prognosis of patients. RBPs are considered to be regulatory components of driving oncogenic mutations [40]. Numerous studies have implicated RBPs in the initiation, progression, and outcomes of malignant tumors [15, 41-43]. On the other hand, prognostic signatures constructed based on RBPs perform well in predicting the survival rate of osteosarcoma [44]. RBM34 is a member of the RBM family and its oncogenic function in HCC has been validated by *in vitro* and *in vivo* experiments. In addition, high expression of RBM34 is associated with poorer prognosis and clinicopathologic features of HCC [28].

However, the role of RBM34 in osteosarcoma and the modeling of its prognostic effects have not been explored and constructed. We evaluated the association of RBM34 with the immune microenvironment and clinical significance of osteosarcoma and further elucidated its potential mechanism of action.

In this study, we first used the TIMER, TCGA, TARGET, and GTEx databases and found that RBM34 was differentially expressed in most human cancers, including osteosarcoma. Consistent with previous studies, Wang et al. determined that RBM34 was highly expressed in HCC tissues and promoted proliferation, migration, and invasion of HCC cells while inhibiting apoptosis [28]. Subsequently, the subcellular localization of the RBM34 protein was examined, and it was found to be predominantly localized in the nucleus, which is consistent with the functional properties of RBM34 as an RNA-binding protein. We also investigated the correlation between RBM34 and different pathological stages and revealed that the expression of RBM34 varied significantly across stages in KICH, KIRC, LIHC, MESO, STAD, and READ. For example, in MESO and STAD, RBM34 is more abundantly expressed in stages I, II, and III than in stage IV. Conversely, in KICH and LIHC, RBM34 expression was elevated in stage IV compared with other stages, suggesting that RBM34 may disparately contribute to tumor progression. The search for early diagnostic markers of cancer is clinically essential and assists in optimizing the clinical prospects of patients. We explored the prognostic value of RBM34 in various cancers by Kaplan-Meier survival analysis and discovered that upregulation of RBM34 expression was associated with poor DSS in ACC, UCEC, and KIRC. However, high expression of RBM34 was related to superior DSS in LGG. These results suggest that RBM34 may exert distinct prognostic utility in different tumors. The nomogram is more accurate than traditional staging systems in predicting prognosis for various cancers by predicting the likelihood of an outcome event based on the patient's personal data [45]. To further

RBM34 as a potential biomarker for osteosarcoma

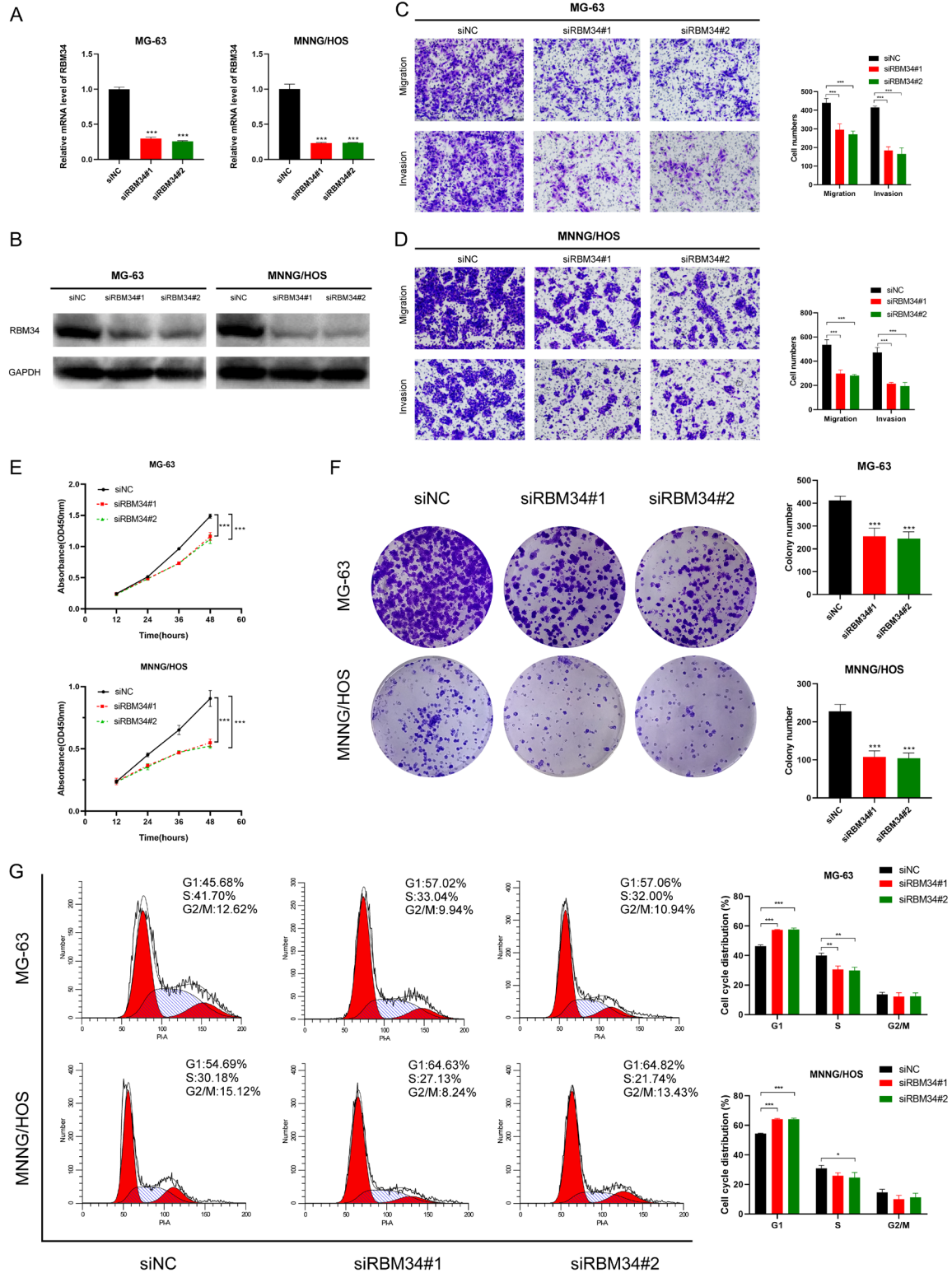


Figure 9. RBM34 accelerated the progression and metastasis of osteosarcoma. (A, B) The mRNA (A) and protein (B) expression levels of osteosarcoma cells after transfecting RBM34-specific siRNAs. (C, D) Migration and invasion of MG-63 (C) and MNNG/HOS (D) cells after transfecting RBM34-specific siRNAs (magnification, 100 ×). (E, F) CCK8 (E) and clone formation assays (F) of osteosarcoma cells after transfecting RBM34-specific siRNAs. (G) The cell cycle distribution of si-RBM34 MG-63 and MNNG/HOS cells by Flow cytometry analysis.

RBM34 as a potential biomarker for osteosarcoma

enhance the value and credibility of RBM34 in clinical applications, a nomogram was constructed using RBM34 and various clinical characteristics to assess individual survival risk, and the calibration curves demonstrated the accurate predictive ability of the nomogram. Overall, we systematically investigated the expression, subcellular localization, and prognostic value of RBM34 in pan-cancer and osteosarcoma, suggesting its promising clinical application.

The tumor microenvironment is a product of the dynamic interplay between various cellular and non-cellular components [46]. It is not a solitary bystander, but rather a collective of performers, including cancer cells, fibroblasts, endothelial cells, and immune cells [47]. Each cancer type has unique molecular features and TME, which may lead to alterations in RBM34 expression. Therefore, it is necessary to further evaluate the interaction of RBM34 with the TME and immune response. ESTIMATE analysis revealed significant positive correlations between RBM34 expression and immune score in KICH and THYM, while in CHOL and LGG, RBM34 expression was significantly negatively correlated with stromal scores. Immune cells have been implicated as critical subpopulations regulating malignancy progression within the TME, which may influence the clinical efficacy of immunotherapy and constitute an independent prognostic factor for cancer patients [48-52]. Using the TISIDB database, we investigated the correlation between RBM34 and immune cell subtypes, immunostimulators, immunoinhibitors, chemokines, and chemokine receptors in 30 tumor types. On the other hand, we discovered that in osteosarcoma, RBM34 expression displayed a positive correlation with infiltrating resting memory CD4⁺ T cells and activated NK cells, and a negative correlation with $\gamma\delta$ T cell abundance by applying the CIBERSORT algorithm. NK cells typically secrete cytokines and chemokines and could directly recognize and kill tumor cells without antigen presentation [53]. CAR-NK cells are attractive and promising for clinical research based on their potent selective anti-tumor efficacy and immunosurveillance capabilities [54]. $\gamma\delta$ T cells exhibit direct cytotoxicity against various types of cancer cells and could activate immunity along with other effector cells to eliminate tumors [55]. Likewise, it has gained

increasing traction in CAR-T cell immunotherapy [56]. Interestingly, ICIs might promote $\gamma\delta$ T cell activation and synergistic antitumor effects by targeting immune checkpoints to reverse $\gamma\delta$ T cell dysfunction in the TME [57]. Evidently, either NK cells or $\gamma\delta$ T cells are appealing candidates for antitumor therapy. Overall, the aforementioned findings indicated that RBM34 may engage in the malignant advancement of tumors by influencing TME.

This study also examined the association of RBM34 with TMB, MSI, MMR, and tumor stemness indicators, which are currently considered to be strong biomarkers for predicting ICI response [34]. For multiple cancers, higher TMB was related to improved survival after immunotherapy [58]. Furthermore, ICIs are highly effective in the treatment of MSI-high status or mismatch repair-deficient tumors [59, 60]. Our results demonstrated that RBM34 expression negatively correlated with TMB and MSI in SARC, while positively correlated with TMB and MSI in BRCA, READ, HNSC, and COAD. These results suggest that BRCA, READ, HNSC, and COAD patients with high RBM34 expression have higher immunogenicity and may be potential high-benefit populations for ICB therapy. Furthermore, RBM34 is tightly related to eight ICGs and three HLA genes in osteosarcoma, which may provide a valuable reference for targeting RBM34 to enhance immunotherapy. Regarding the pharmacogenomic features of RBM34 in osteosarcoma, patients with high RBM34 expression were more responsive to AICAR, Camptothecin, Cisplatin, and Mitomycin.C. Conversely, Bexarotene, BI.2536, Bicalutamide, CGP.60474, DMOG, FTI.277, GNF.2, GSK269962A, JW.7.52.1, KIN001.135, Lapatinib, NVP.TAE684, PF.02341066, PHA.665752, Roscovitine, and Shikonin had lower IC50 values in the low RBM34 expression subgroup. Of course, these results should be further validated by additional experimental studies and clinical trials. Among these small molecule candidates, AICAR has been reported to reduce the growth of EGFR mutant tumor cells by inducing DNA damage and apoptosis [61]. Its combination with the chemotherapeutic agent topotecan reduced retinoblastoma progression with minimal retinal damage [62]. Camptothecin is a broad-spectrum anticancer agent that specifically targets DNA topoisomerase I [63]. Its derivative, irinotecan, is approved for the com-

ination treatment of metastatic or advanced solid tumors, including colorectal, gastric and pancreatic cancers [64]. Bexarotene, a retinoid X receptor agonist, exerts its growth-inhibitory and differentiation-inducing effects on cancer cells in vitro and vivo and also reduces tumor cell migration and invasion in a dose-dependent manner [65]. Based on these studies, it is reasonable to hypothesize that targeting RBM34 may provide appropriate immunotherapeutic and chemotherapeutic strategies.

To further explore the biological activities of RBM34, enrichment analyses of RBM34-derived differential genes were performed. The results indicated that RBM34 may affect tumorigenesis in pan-cancer by regulating various cellular processes, including invasion, DNA repair, DNA damage, stemness, metastasis, and apoptosis. Next, we constructed an RBM34-derived genomic prognostic signature based on six RRDEGs (FAM81A, BBS4, FBXL5, LBR, SYNGAP1, and ZNF610). Grouping based on the median RDPI score revealed that the survival of the high RDPI score subgroup was significantly inferior to that of the low RDPI score subgroup. The ROC curves suggested that the RDPI score had good sensitivity and specificity in predicting OS in osteosarcoma. Meanwhile, multivariate Cox regression suggested that the RDPI score could be used as an independent prognostic factor for osteosarcoma patients. In the subgroup analysis of different clinical characteristics, the probability of metastasis was higher in patients with high RDPI scores. CAF is valuable in immune dysregulation, tumor diagnosis, and prognostic evaluation as one of the major stromal cells in the TME. Synthesizing the ESTIMATE, MCPCounter, xCELL, and EPIC algorithms, the patients with high RDPI scores had low CAF abundance and stromal scores but high tumor purity. To some extent, this explains the poor clinical outcomes in the high RDPI score subgroup. Among these six RRDEGs, FBXL5 mediated post-translational downregulation of Snail during GPER activation in osteosarcoma [66]. Unfortunately, the remaining five RRDEGs have hardly been reported in osteosarcoma. However, these RRDEGs have demonstrated function in other cancers. For instance, LBR is critical for maintaining chromosome stability, and its deletion induces mitotic defects, nuclear aberrations, and increased tumorigenicity [67].

Additionally, ZNF610 has been identified as a DNA methylation biomarker for HNSC diagnosis and progression of human gastric lesions and also negatively correlated with progression-free survival in castration-resistant prostate cancer [68-70]. Furthermore, since BBS4 contributes to the preservation of normal organelle homeostasis, NRF2 could inhibit primary cilia formation and promote tumor progression by suppressing the ciliary entry of BBS4 [71]. Finally, we examined the biological activity of RBM34 in osteosarcoma cells. RBM34 silencing induced G1 cell cycle arrest and suppressed growth, migration, and invasion of MG-63 and MNNG/HOS cells, which is consistent with recent studies on HCC [28].

Post-transcriptional regulation is a dynamic and continuous process, and the reflection of the function of RBPs still needs further mechanistic exploration; therefore, this study has some limitations. First, the RBM34-derived prognostic index needs to be validated in a prospective multicenter cohort. Second, further in vitro and in vivo experimental studies are needed to elucidate the molecular mechanisms involved for better clinical practice.

Conclusion

In conclusion, the present study was systematically explored using multi-omics data to reveal the close association between RBM34 expression and pan-cancer clinical outcome, tumor microenvironment, tumor stemness, and immunotherapy response, which helped us in clinical stratification management. Meanwhile, bioinformatics and in vitro experiments demonstrated that RBM34 significantly promoted osteosarcoma proliferation and migration, suggesting its potential role as a therapeutic target.

Acknowledgements

This work was supported by the National Natural Science Foundation of China (8160-1931), the Natural Science Foundation of Jiangsu Province (BK20150475), the Youth Medical Key Talent Project of Jiangsu (QNRC-2016844), and "Six One Projects" for high-level health professionals in Jiangsu Province Top Talent Project (LGY2019089).

Disclosure of conflict of interest

None.

Address correspondence to: Dapeng Li and Yiming Zhang, Affiliated Hospital of Jiangsu University, Zhenjiang 212000, Jiangsu, China. E-mail: lidapeng706@hotmail.com (DPL); zhangyiming0607@163.com (YMZ); Qiping Zheng, Department of Hematological Laboratory Science, Jiangsu Key Laboratory of Medical Science and Laboratory Medicine, School of Medicine, Jiangsu University, Zhenjiang 212000, Jiangsu, China. E-mail: qp_zheng@hotmail.com

References

- [1] Zhu K, Liu L, Zhang J, Wang Y, Liang H, Fan G, Jiang Z, Zhang CY, Chen X and Zhou G. MiR-29b suppresses the proliferation and migration of osteosarcoma cells by targeting CDK6. *Protein Cell* 2016; 7: 434-444.
- [2] Whelan JS, Jinks RC, McTiernan A, Sydes MR, Hook JM, Trani L, Uscinska B, Bramwell V, Lewis IJ, Nooij MA, van Glabbeke M, Grimer RJ, Hogendoorn PC, Taminiou AH and Gelderblom H. Survival from high-grade localised extremity osteosarcoma: combined results and prognostic factors from three European Osteosarcoma Intergroup randomised controlled trials. *Ann Oncol* 2012; 23: 1607-1616.
- [3] Kunz P, Fellenberg J, Moskovszky L, Sapi Z, Krenacs T, Machado I, Poeschl J, Lehner B, Szendroi M, Ruef P, Bohlmann M, Bosch AL, Ewerbeck V, Kinscherf R and Fritzsching B. Improved survival in osteosarcoma patients with atypical low vascularization. *Ann Surg Oncol* 2015; 22: 489-496.
- [4] Zhang Y, Gan W, Ru N, Xue Z, Chen W, Chen Z, Wang H and Zheng X. Comprehensive multi-omics analysis reveals m7G-related signature for evaluating prognosis and immunotherapy efficacy in osteosarcoma. *J Bone Oncol* 2023; 40: 100481.
- [5] Zhang Y, Ning R, Wang W, Zhou Y and Chen Y. Synthesis of Fe(3)O(4)/PDA nanocomposites for osteosarcoma magnetic resonance imaging and photothermal therapy. *Front Bioeng Biotechnol* 2022; 10: 844540.
- [6] Anwar MA, El-Baba C, Elnaggar MH, Elkholy YO, Mottawea M, Johar D, Al Shehabi TS, Kobeissy F, Moussalem C, Massaad E, Omeis I, Darwiche N and Eid AH. Novel therapeutic strategies for spinal osteosarcomas. *Semin Cancer Biol* 2020; 64: 83-92.
- [7] Zhang K, Dong C, Chen M, Yang T, Wang X, Gao Y, Wang L, Wen Y, Chen G, Wang X, Yu X, Zhang Y, Wang P, Shang M, Han K and Zhou Y. Extracellular vesicle-mediated delivery of miR-101 inhibits lung metastasis in osteosarcoma. *Theranostics* 2020; 10: 411-425.
- [8] Kuo HM, Tseng CC, Chen NF, Tai MH, Hung HC, Feng CW, Cheng SY, Huang SY, Jean YH and Wen ZH. MSP-4, an antimicrobial peptide, induces apoptosis via activation of extrinsic Fas/FasL- and intrinsic mitochondria-mediated pathways in one osteosarcoma cell line. *Mar Drugs* 2018; 16: 8.
- [9] Corre I, Verrecchia F, Crenn V, Redini F and Trichet V. The osteosarcoma microenvironment: a complex but targetable ecosystem. *Cells* 2020; 9: 976.
- [10] Heymann MF, Lezot F and Heymann D. The contribution of immune infiltrates and the local microenvironment in the pathogenesis of osteosarcoma. *Cell Immunol* 2019; 343: 103711.
- [11] Huang Q, Liang X, Ren T, Huang Y, Zhang H, Yu Y, Chen C, Wang W, Niu J, Lou J and Guo W. The role of tumor-associated macrophages in osteosarcoma progression - therapeutic implications. *Cell Oncol (Dordr)* 2021; 44: 525-539.
- [12] Panez-Toro I, Munoz-Garca J, Vargas-Franco JW, Renodon-Corniere A, Heymann MF, Lezot F and Heymann D. Advances in osteosarcoma. *Curr Osteoporos Rep* 2023; 21: 330-343.
- [13] Clemente O, Ottaiano A, Di Lorenzo G, Bracigliano A, Lamia S, Cannella L, Pizzolorusso A, Di Marzo M, Santorsola M, De Chiara A, Fazioli F and Tafuto S. Is immunotherapy in the future of therapeutic management of sarcomas? *J Transl Med* 2021; 19: 173.
- [14] Varesi A, Campagnoli LIM, Barbieri A, Rossi L, Ricevuti G, Esposito C, Chirumbolo S, Marchesi N and Pascale A. RNA binding proteins in senescence: a potential common linker for age-related diseases? *Ageing Res Rev* 2023; 88: 101958.
- [15] Bertoldo JB, Muller S and Huttelmaier S. RNA-binding proteins in cancer drug discovery. *Drug Discov Today* 2023; 28: 103580.
- [16] Cen Y, Chen L, Liu Z, Lin Q, Fang X, Yao H and Gong C. Novel roles of RNA-binding proteins in drug resistance of breast cancer: from molecular biology to targeting therapeutics. *Cell Death Discov* 2023; 9: 52.
- [17] Nag S, Goswami B, Das Mandal S and Ray PS. Cooperation and competition by RNA-binding proteins in cancer. *Semin Cancer Biol* 2022; 86: 286-297.
- [18] Zhao Y, Mir C, Garcia-Mayea Y, Paciucci R, Kondoh H and LLeonart ME. RNA-binding proteins: underestimated contributors in tumorigenesis. *Semin Cancer Biol* 2022; 86: 431-444.
- [19] Elcheva IA, Gowda CP, Bogush D, Gornostaeva S, Fakhardo A, Sheth N, Kokolus KM, Sharma A, Dovat S, Uzun Y, Schell TD and Spiegelman VS. IGF2BP family of RNA-binding proteins regulate innate and adaptive immune responses in cancer cells and tumor microenvironment. *Front Immunol* 2023; 14: 1224516.
- [20] Qin H, Ni H, Liu Y, Yuan Y, Xi T, Li X and Zheng L. RNA-binding proteins in tumor progression. *J Hematol Oncol* 2020; 13: 90.

RBM34 as a potential biomarker for osteosarcoma

- [21] Li W, Deng X and Chen J. RNA-binding proteins in regulating mRNA stability and translation: roles and mechanisms in cancer. *Semin Cancer Biol* 2022; 86: 664-677.
- [22] Wu X and Xu L. The RNA-binding protein HuR in human cancer: a friend or foe? *Adv Drug Deliv Rev* 2022; 184: 114179.
- [23] Schultz CW, Preet R, Dhir T, Dixon DA and Brody JR. Understanding and targeting the disease-related RNA binding protein human antigen R (HuR). *Wiley Interdiscip Rev RNA* 2020; 11: e1581.
- [24] Li Z, Guo Q, Zhang J, Fu Z, Wang Y, Wang T and Tang J. The RNA-binding motif protein family in cancer: friend or foe? *Front Oncol* 2021; 11: 757135.
- [25] Bechara EG, Sebestyén E, Bernardis I, Eyraes E and Valcárcel J. RBM5, 6, and 10 differentially regulate NUMB alternative splicing to control cancer cell proliferation. *Mol Cell* 2013; 52: 720-733.
- [26] Xia A, Yue Q, Zhu M, Xu J, Liu S, Wu Y, Wang Z, Xu Z, An H, Wang Q, Wang S and Sun B. The cancer-testis lncRNA LINC01977 promotes HCC progression by interacting with RBM39 to prevent Notch2 ubiquitination. *Cell Death Discov* 2023; 9: 169.
- [27] Sun X, Hu Y, Wu J, Shi L, Zhu L, Xi PW, Wei JF and Ding Q. RBMS2 inhibits the proliferation by stabilizing P21 mRNA in breast cancer. *J Exp Clin Cancer Res* 2018; 37: 298.
- [28] Wang W, Zhang R, Feng N, Zhang L and Liu N. Overexpression of RBM34 promotes tumor progression and correlates with poor prognosis of hepatocellular carcinoma. *J Clin Transl Hepatol* 2023; 11: 369-381.
- [29] Zhang Y, He R, Lei X, Mao L, Yin Z, Zhong X, Cao W, Zheng Q and Li D. Comprehensive analysis of a ferroptosis-related lncRNA signature for predicting prognosis and immune landscape in osteosarcoma. *Front Oncol* 2022; 12: 880459.
- [30] Thanindrarn P, Wei R, Dean DC, Singh A, Felderman N, Nelson SD, Hornicek FJ and Duan Z. T-LAK cell-originated protein kinase (TOPK): an emerging prognostic biomarker and therapeutic target in osteosarcoma. *Mol Oncol* 2021; 15: 3721-3737.
- [31] Yarchoan M, Hopkins A and Jaffee EM. Tumor mutational burden and response rate to PD-1 inhibition. *N Engl J Med* 2017; 377: 2500-2501.
- [32] Overman MJ, McDermott R, Leach JL, Lonardi S, Lenz HJ, Morse MA, Desai J, Hill A, Axelson M, Moss RA, Goldberg MV, Cao ZA, Ledine JM, Maglente GA, Kopetz S and André T. Nivolumab in patients with metastatic DNA mismatch repair-deficient or microsatellite instability-high colorectal cancer (CheckMate 142): an open-label, multicentre, phase 2 study. *Lancet Oncol* 2017; 18: 1182-1191.
- [33] Morse MA, Overman MJ, Hartman L, Khoukatz T, Brutcher E, Lenz HJ, Atasoy A, Shangguan T, Zhao H and El-Rayes B. Safety of nivolumab plus low-dose ipilimumab in previously treated microsatellite instability-high/mismatch repair-deficient metastatic colorectal cancer. *Oncologist* 2019; 24: 1453-1461.
- [34] He R, Zhang H, Zhao H, Yin X, Lu J, Gu C, Gao J and Xu Q. Multiomics analysis reveals cuproptosis-related signature for evaluating prognosis and immunotherapy efficacy in colorectal cancer. *Cancers (Basel)* 2023; 15: 387.
- [35] Yuan H, Yan M, Zhang G, Liu W, Deng C, Liao G, Xu L, Luo T, Yan H, Long Z, Shi A, Zhao T, Xiao Y and Li X. CancerSEA: a cancer single-cell state atlas. *Nucleic Acids Res* 2019; 47: D900-D908.
- [36] Perleberg C, Kind A and Schnieke A. Genetically engineered pigs as models for human disease. *Dis Model Mech* 2018; 11: dmm030783.
- [37] Zi X, Zhang G and Qiu S. Up-regulation of LINC00619 promotes apoptosis and inhibits proliferation, migration and invasion while promoting apoptosis of osteosarcoma cells through inactivation of the HGF-mediated PI3K-Akt signalling pathway. *Epigenetics* 2022; 17: 147-160.
- [38] Chen Y, Liu R, Wang W, Wang C, Zhang N, Shao X, He Q and Ying M. Advances in targeted therapy for osteosarcoma based on molecular classification. *Pharmacol Res* 2021; 169: 105684.
- [39] Zhang Y, He R, Lei X, Mao L, Jiang P, Ni C, Yin Z, Zhong X, Chen C, Zheng Q and Li D. A novel pyroptosis-related signature for predicting prognosis and indicating immune microenvironment features in osteosarcoma. *Front Genet* 2021; 12: 780780.
- [40] Hopkins TG, Mura M, Al-Ashtal HA, Lahr RM, Abd-Latip N, Sweeney K, Lu H, Weir J, El-Bahrawy M, Steel JH, Ghaem-Maghami S, Aboagye EO, Berman AJ and Blagden SP. The RNA-binding protein LARP1 is a post-transcriptional regulator of survival and tumorigenesis in ovarian cancer. *Nucleic Acids Res* 2016; 44: 1227-1246.
- [41] Aguilar-Garrido P, Otero-Sobrinho Á, Navarro-Aguadero MÁ, Velasco-Estévez M and Gallardo M. The role of RNA-binding proteins in hematological malignancies. *Int J Mol Sci* 2022; 23: 9552.
- [42] Mehta M, Raguraman R, Ramesh R and Munshi A. RNA binding proteins (RBPs) and their role in DNA damage and radiation response in cancer. *Adv Drug Deliv Rev* 2022; 191: 114569.

RBM34 as a potential biomarker for osteosarcoma

- [43] Choi PS and Thomas-Tikhonenko A. RNA-binding proteins of COSMIC importance in cancer. *J Clin Invest* 2021; 131: e151627.
- [44] Gul Mohammad A, Li D, He R, Lei X, Mao L, Zhang B, Zhong X, Yin Z, Cao W, Zhang W, Hei R, Zheng Q and Zhang Y. Integrated analyses of an RNA binding protein-based signature related to tumor immune microenvironment and candidate drugs in osteosarcoma. *Am J Transl Res* 2022; 14: 2501-2526.
- [45] Gu D, Zheng R, Xin J, Li S, Chu H, Gong W, Qiang F, Zhang Z, Wang M, Du M and Chen J. Evaluation of GWAS-identified genetic variants for gastric cancer survival. *EBioMedicine* 2018; 33: 82-87.
- [46] Schaaf MB, Garg AD and Agostinis P. Defining the role of the tumor vasculature in antitumor immunity and immunotherapy. *Cell Death Dis* 2018; 9: 115.
- [47] Singh S, Ray LA, Shahi Thakuri P, Tran S, Konopka MC, Luker GD and Tavana H. Organotypic breast tumor model elucidates dynamic remodeling of tumor microenvironment. *Biomaterials* 2020; 238: 119853.
- [48] Zhang X, Xie J, He D, Yan X and Chen J. Cell pair algorithm-based immune infiltrating cell signature for improving outcomes and treatment responses in patients with hepatocellular carcinoma. *Cells* 2023; 12: 202.
- [49] Wistuba-Hamprecht K, Martens A, Haehnel K, Geukes Foppen M, Yuan J, Postow MA, Wong P, Romano E, Khammari A, Dreno B, Capone M, Ascierto PA, Demuth I, Steinhagen-Thiessen E, Larbi A, Schilling B, Schadendorf D, Wolchok JD, Blank CU, Pawelec G, Garbe C and Weide B. Proportions of blood-borne V δ 1+ and V δ 2+ T-cells are associated with overall survival of melanoma patients treated with ipilimumab. *Eur J Cancer* 2016; 64: 116-126.
- [50] Badoual C, Hans S, Rodriguez J, Peyrard S, Klein C, Agueznay Nel H, Mosseri V, Laccourreye O, Bruneval P, Fridman WH, Brasnu DF and Tartour E. Prognostic value of tumor-infiltrating CD4+ T-cell subpopulations in head and neck cancers. *Clin Cancer Res* 2006; 12: 465-472.
- [51] Carreras J, Lopez-Guillermo A, Fox BC, Colomo L, Martinez A, Roncador G, Montserrat E, Campo E and Banham AH. High numbers of tumor-infiltrating FOXP3-positive regulatory T cells are associated with improved overall survival in follicular lymphoma. *Blood* 2006; 108: 2957-2964.
- [52] Bense RD, Sotiriou C, Piccart-Gebhart MJ, Haanen JBAG, van Vugt MATM, de Vries EGE, Schröder CP and Fehrmann RSN. Relevance of tumor-infiltrating immune cell composition and functionality for disease outcome in breast cancer. *J Natl Cancer Inst* 2016; 109: djw192.
- [53] Deng W, Gowen BG, Zhang L, Wang L, Lau S, Iannello A, Xu J, Rovis TL, Xiong N and Raulet DH. Antitumor immunity. A shed NKG2D ligand that promotes natural killer cell activation and tumor rejection. *Science* 2015; 348: 136-139.
- [54] Zhang H, Yang L, Wang T and Li Z. NK cell-based tumor immunotherapy. *Bioact Mater* 2023; 31: 63-86.
- [55] Ma L, Feng Y and Zhou Z. A close look at current $\gamma\delta$ T-cell immunotherapy. *Front Immunol* 2023; 14: 1140623.
- [56] Park JH and Lee HK. Function of $\gamma\delta$ T cells in tumor immunology and their application to cancer therapy. *Exp Mol Med* 2021; 53: 318-327.
- [57] Gao Z, Bai Y, Lin A, Jiang A, Zhou C, Cheng Q, Liu Z, Chen X, Zhang J and Luo P. Gamma delta T-cell-based immune checkpoint therapy: attractive candidate for antitumor treatment. *Mol Cancer* 2023; 22: 31.
- [58] Samstein RM, Lee CH, Shoushtari AN, Hellmann MD, Shen R, Janjigian YY, Barron DA, Zehir A, Jordan EJ, Omuro A, Kaley TJ, Kendall SM, Motzer RJ, Hakimi AA, Voss MH, Russo P, Rosenberg J, Iyer G, Bochner BH, Bajorin DF, Al-Ahmadie HA, Chaft JE, Rudin CM, Riely GJ, Baxi S, Ho AL, Wong RJ, Pfister DG, Wolchok JD, Barker CA, Gutin PH, Brennan CW, Tabar V, Mellinger IK, DeAngelis LM, Ariyan CE, Lee N, Tap WD, Gounder MM, D'Angelo SP, Saltz L, Stadler ZK, Scher HI, Baselga J, Razavi P, Klebanoff CA, Yaeger R, Segal NH, Ku GY, DeMatteo RP, Ladanyi M, Rizvi NA, Berger MF, Riaz N, Solit DB, Chan TA and Morris LGT. Tumor mutational load predicts survival after immunotherapy across multiple cancer types. *Nat Genet* 2019; 51: 202-206.
- [59] Le DT, Uram JN, Wang H, Bartlett BR, Kemberling H, Eyring AD, Skora AD, Luber BS, Azad NS, Laheru D, Biedrzycki B, Donehower RC, Zaheer A, Fisher GA, Crocenzi TS, Lee JJ, Duffy SM, Goldberg RM, de la Chapelle A, Koshiji M, Bhajee F, Huebner T, Hruban RH, Wood LD, Cuka N, Pardoll DM, Papadopoulos N, Kinzler KW, Zhou S, Cornish TC, Taube JM, Anders RA, Eshleman JR, Vogelstein B and Diaz LA Jr. PD-1 blockade in tumors with mismatch-repair deficiency. *N Engl J Med* 2015; 372: 2509-2520.
- [60] Le DT, Durham JN, Smith KN, Wang H, Bartlett BR, Aulakh LK, Lu S, Kemberling H, Wilt C, Luber BS, Wong F, Azad NS, Rucki AA, Laheru D, Donehower R, Zaheer A, Fisher GA, Crocenzi TS, Lee JJ, Greten TF, Duffy AG, Ciombor KK, Eyring AD, Lam BH, Joe A, Kang SP, Holdhoff M, Danilova L, Cope L, Meyer C, Zhou S, Goldberg RM, Armstrong DK, Bever KM, Fader AN, Taube J, Housseau F, Spetzler D, Xiao N, Pardoll DM, Papadopoulos N, Kinzler KW, Eshleman JR, Vogelstein B, Anders RA and Diaz LA

RBM34 as a potential biomarker for osteosarcoma

- Jr. Mismatch repair deficiency predicts response of solid tumors to PD-1 blockade. *Science* 2017; 357: 409-413.
- [61] Aftab F, Rodriguez-Fuguet A, Silva L, Kobayashi IS, Sun J, Politi K, Levantini E, Zhang W, Kobayashi SS and Zhang WC. An intrinsic purine metabolite AICAR blocks lung tumour growth by targeting oncoprotein mucin 1. *Br J Cancer* 2023; 128: 1647-1664.
- [62] Babu VS, Mallipatna A, Dudeja G, Shetty R, Nair AP, Tun SBB, Ho CEH, Chaurasia SS, Bhattacharya SS, Verma NK, Lakshminarayanan R, Guha N, Heymans S, Barathi VA and Ghosh A. Depleted hexokinase1 and lack of AMPK α activation favor OXPHOS-dependent energetics in retinoblastoma tumors. *Transl Res* 2023; 261: 41-56.
- [63] Pommier Y. Topoisomerase I inhibitors: camptothecins and beyond. *Nat Rev Cancer* 2006; 6: 789-802.
- [64] Bailly C. Irinotecan: 25 years of cancer treatment. *Pharmacol Res* 2019; 148: 104398.
- [65] Qu L and Tang X. Bexarotene: a promising anticancer agent. *Cancer Chemother Pharmacol* 2010; 65: 201-205.
- [66] Wang Z, Chen X, Zhao Y, Jin Y and Zheng J. G-protein-coupled estrogen receptor suppresses the migration of osteosarcoma cells via post-translational regulation of Snail. *J Cancer Res Clin Oncol* 2019; 145: 87-96.
- [67] Patil S, Deshpande S and Sengupta K. Nuclear envelope protein lamin B receptor protects the genome from chromosomal instability and tumorigenesis. *Hum Mol Genet* 2023; 32: 745-763.
- [68] Zhou C, Ye M, Ni S, Li Q, Ye D, Li J, Shen Z and Deng H. DNA methylation biomarkers for head and neck squamous cell carcinoma. *Epigenetics* 2018; 13: 398-409.
- [69] Schneider BG, Mera R, Piazuelo MB, Bravo JC, Zabaleta J, Delgado AG, Bravo LE, Wilson KT, El-Rifai W, Peek RM Jr and Correa P. DNA methylation predicts progression of human gastric lesions. *Cancer Epidemiol Biomarkers Prev* 2015; 24: 1607-1613.
- [70] Pudova EA, Krasnov GS, Kobelyatskaya AA, Savvateeva MV, Fedorova MS, Pavlov VS, Nyushko KM, Kaprin AD, Alekseev BY, Trofimov DY, Sukhikh GT, Snezhkina AV and Kudryavtseva AV. Gene expression changes and associated pathways involved in the progression of prostate cancer advanced stages. *Front Genet* 2020; 11: 613162.
- [71] Liu P, Dodson M, Fang D, Chapman E and Zhang DD. NRF2 negatively regulates primary ciliogenesis and hedgehog signaling. *PLoS Biol* 2020; 18: e3000620.

RBM34 as a potential biomarker for osteosarcoma

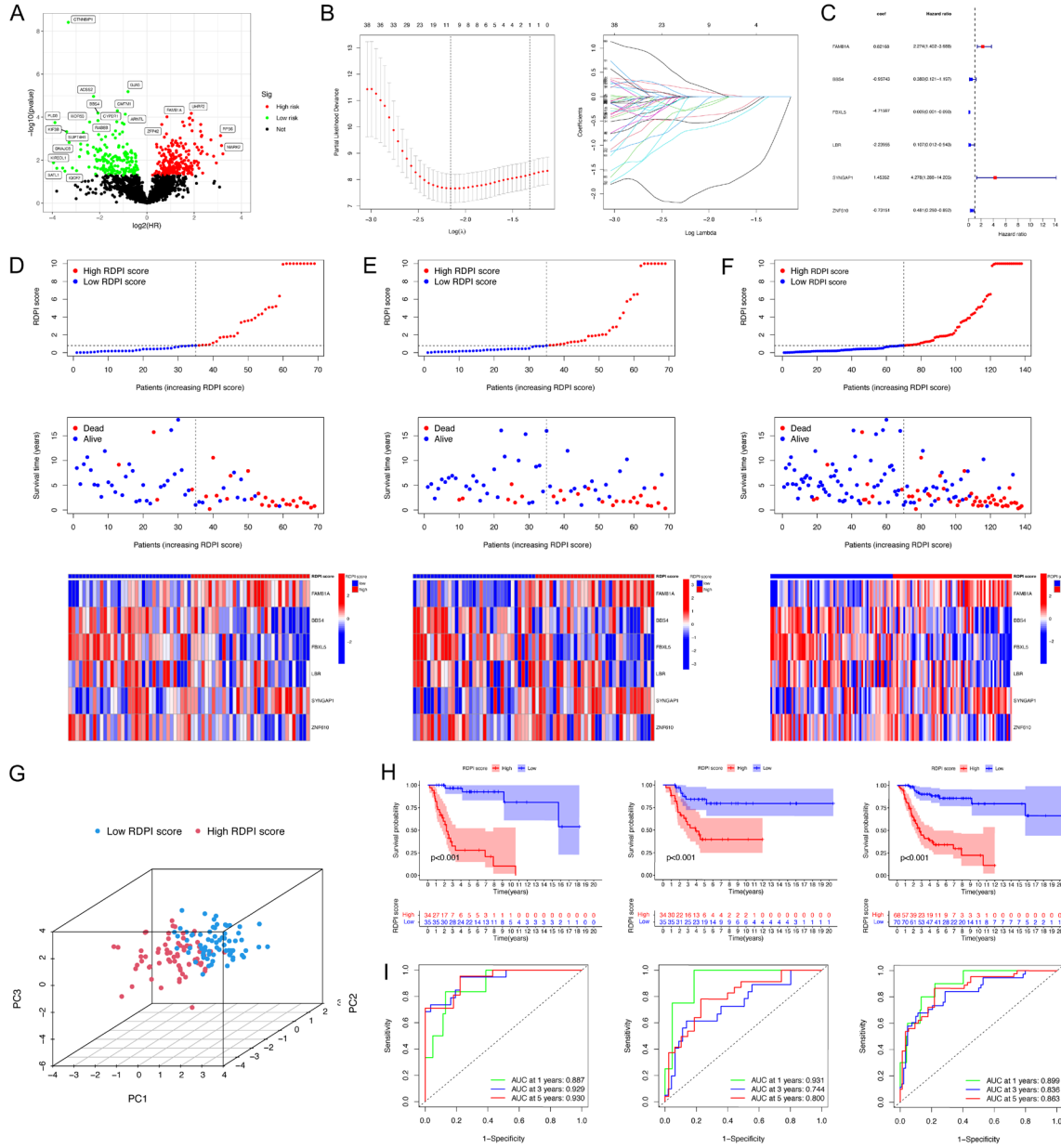
Supplementary Table 1. The abbreviations and corresponding full names of 33 cancer types

Cancer Type	Abbreviation
adrenocortical carcinoma	ACC
bladder urothelial carcinoma	BLCA
breast invasive carcinoma	BRCA
cervical squamous cell carcinoma and endocervical adenocarcinoma	CESC
cholangiocarcinoma	CHOL
colon adenocarcinoma	COAD
lymphoid neoplasm diffuse Large B-cell lymphoma	DLBC
esophageal carcinoma	ESCA
glioblastoma multiforme	GBM
head and neck squamous cell carcinoma	HNSC
kidney chromophobe	KICH
kidney renal clear cell carcinoma	KIRC
kidney renal papillary cell carcinoma	KIRP
acute myeloid leukemia	LAML
brain lower grade glioma	LGG
liver hepatocellular carcinoma	LIHC
lung adenocarcinoma	LUAD
lung squamous cell carcinoma	LUSC
mesothelioma	MESO
ovarian serous cystadenocarcinoma	OV
pancreatic adenocarcinoma	PAAD
pheochromocytoma and paraganglioma	PCPG
prostate adenocarcinoma	PRAD
rectum adenocarcinoma	READ
sarcoma	SARC
skin cutaneous melanoma	SKCM
stomach adenocarcinoma	STAD
testicular germ cell tumors	TGCT
thyroid carcinoma	THCA
thymoma	THYM
uterine corpus endometrial carcinoma	UCEC
uterine carcinosarcoma	UCS
uveal melanoma	UVM

Supplementary Table 2. Primers for qRT-PCR and small interfering RNAs

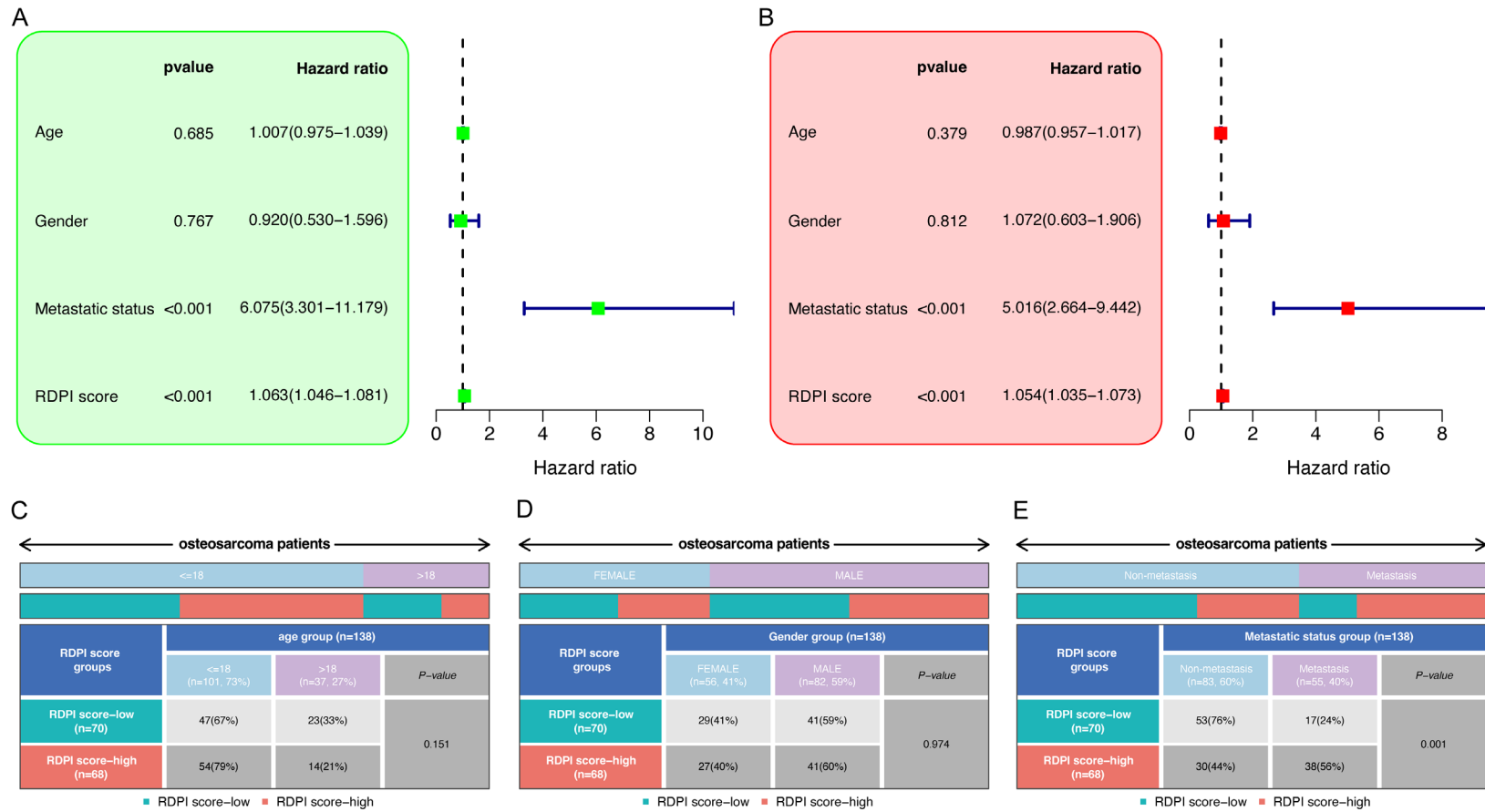
Primers		Sequence (5'-3')
RBM34	F	ATGGCCTTGAAGGGATGAG
	R	GAACGCCGTCGTCAGGATT
GAPDH	F	AAGCCCATCACCATCTTCCA
	R	TAGACTCCACGACATACTCA
siRBM34#1	F	GAAGCACUUUCUGACUGUTT
	R	ACAGUCCAGAAAGUGCUUCTT
siRBM34#2	F	GAUUGCAGAUUGAUUUCGUTT
	R	ACGAAAUCCAUCUGCAAUCTT
siNC	F	UUCUCCGAACGUGUCACGUTT
	R	ACGUGACACGUUCGGAGAATT

RBM34 as a potential biomarker for osteosarcoma



Supplementary Figure 1. Construction of RBM34-derived genomic prognostic signature in osteosarcoma. (A) Volcano plot of the prognosis-related RRDEGs by univariable Cox regression analysis. (B, C) LASSO (B) and multivariate (C) Cox regression analysis for constructing the RDPI in osteosarcoma. (D-F) The RDPI score distribution and RRDEGs expression of osteosarcoma patients in the train (D) and validation (E), and entire (F) cohort. (G) Principal component analysis plot of the osteosarcoma cohort. (H) Kaplan-Meier survival curves for osteosarcoma patients in the three cohorts. (I) ROC curves for 1-, 3-, and 5-year survival in the three cohorts. RRDEGs, RBM34-related differentially expressed genes; RDPI, RBM34-derived prognostic index.

RBM34 as a potential biomarker for osteosarcoma



Supplementary Figure 2. Independent prognostic value and clinical correlation analysis. (A, B) Univariate (A) and multivariate (B) independent prognostic analysis of RDPI score and clinical variables. (C-E) Discrepancies in age (C), gender (D), and metastatic status (E) between different RDPI score subgroups.